**Title**
Regulation of G protein-coupled receptors



**Author**
Arden, James,

**Publication Date**
1994

Peer reviewed|Thesis/dissertation

REGULATION OF G PROTEIN-COUPLED RECEPTORS:

MU OPIOID RECEPTOR AND Hm1 MUSCARINIC CHOLINERGIC RECEPTOR

**by**

JAMES ARDEN

B.A., 1971, Columbia University; M.D., 1979, Columbia University

**DISSERTATION**

**Submitted in partial satisfaction of the requirements for the degree of**

**DOCTOR OF PHILOSOPHY**

**in**

Pharmaceutical Chemistry

**in the**

**GRADUATE DIVISION**

**of the**

**UNIVERSITY OF CALIFORNIA**

**San Francisco**

**Date** **University Librarian**

**Degree Conferred:** SEP 4 1994

## PREFACE

This work was performed while I was an Assistant Adjunct Professor of Anesthesia at the University of California, San Francisco. I wished to examine the cell biology of central nervous system G protein-coupled receptors. Initial work on the muscarinic cholinergic receptor was re-directed to the mu-opioid receptor when its cDNA became available to us in the last year. This dissertation presents my work from the most recent findings on the opioid receptor back to the my earlier experiments on muscarinic receptor coupling.

## ACKNOWLEDGMENTS

I would like to thank:

Wolfgang Sadée
Darren Wong
My family: Heidi, Jane, and Peter
Jelveh Lameh
Keith Mostov and the members of his lab
Kathleen Giacomini and the members of her lab
Frances Brodsky and the members of her lab
Friends in the UCSF community who supported and helped me over the past six years

# ABSTRACT

To probe the mechanisms of G protein-coupled receptor (GPCR) regulation following agonist exposure, we first developed a system to isolate and identify two representative GPCRs, the mu-opioid receptor (muR) and the human m1 muscarinic cholinergic receptor (Hm1). An epitope (EYMPME) was appended to the amino terminus by polymerase chain reaction, and the epitope-tagged receptor (EE-R) was stably expressed in HEK 293 cells. Cell expressed 5.5 x $10^6$ EE-muR sites/cell or 4 x $10^5$ EE-Hm1 sites/cell. Detergent solubilized receptors were specifically immunoprecipitated by the corresponding monoclonal antibody. EE-muR and EE-Hm1 were also visualized by immunofluorescence confocal microscopy.

We examined two processes associated with receptor desensitization: agonist induced phosphorylation and agonist-induced internalization. The EE-muR was phosphorylated at rest, and showed a small increase in phosphorylation following 15 minute agonist exposure. By ligand binding and immunofluorescence microscopy, the EE-muR was not internalized during a 19 hour exposure to agonist.

EE-Hm1 was less efficiently solubilized and immunoprecipitated than EE-muR. EE-Hm1 also showed basal phosphorylation which was unchanged by agonist treatment. However, during agonist exposure, EE-Hm1 was seen in numerous cytoplasmic vesicles within five minutes, and vesicles continued to accumulate over the next 40 minutes. An i3-loop deletion mutant of

Hm1 (d232-358), which was internalization-deficient by ligand binding, was seen to internalize more slowly than Hm1. Delayed internalization by EE-Hm1(d232-358) was confirmed on micrographs of synchronized internalization induced by 4°C-37°C temperature shift. An i2-loop double point mutant (V127A/L131A), which was internalization defective by ligand binding, was not visualized in the cytoplasm following agonist treatment.

To determine if the Hm1 i3-loop contained G protein coupling determinants in addition to internalization determinants, deletion- and point-mutants of the i3 loop were tested for intact phosphatidyl inositol hydrolysis. All mutants tested were similar to wild type in coupling, including the d232-358 mutant.

This work establishes a system for the study of G protein coupled receptor regulation and provides physical verification of regulatory processes for two representative GPCRs.

September 2, 1994

# TABLE OF CONTENTS


**PREFACE AND ACKNOWLEDGMENTS** ii

**ABSTRACT** iii

**TABLE OF CONTENTS** v

**LIST OF TABLES** ix

**LIST OF FIGURES** x

**INTRODUCTION**

1. OBJECTIVE 1

2. BACKGROUND 1

2.1 G-protein-Coupled Receptors 1

2.2 Regulation of G protein coupled receptors 4

2.3 Determinants of Receptor Coupling and Internalization 6

**CHAPTER I EPITOPE-TAGGED μ-OPIOID RECEPTOR EXPRESSED IN HUMAN EMBRYONIC KIDNEY (HEK 293) CELLS: CONFOCAL MICROSCOPY, IMMUNOPRECIPITATION AND PHOSPHORYLATION**

1. SUMMARY 8

2. INTRODUCTION 9

3. EXPERIMENTAL PROCEDURES 11
3.1 Materials 11
3.2 Epitope-Tagged μ-Opioid Receptor 12
3.3 Ligand Binding and cAMP Assays 13
3.4 Laser Confocal Microscopy 14
3.5 Receptor Purification and Immunoprecipitation 15
3.6 Immunoprecipitation of the Phosphorylated EE-μR 16
4. RESULTS 17
4.1 Stable Expression in HEK 293 Cells 17
4.2 Confocal Laser Microscopy of EE-μ Opioid Receptor 19
4.3 Purification of EE-μ Opioid Receptor 20
4.4 Phosphorylation of the EE-μ Opioid Receptor 21
5. DISCUSSION 21

**CHAPTER II. PURIFICATION AND IMMUNOPRECIPITATION OF AN EPITOPE-TAGGED HUMAN m1 MUSCARINIC CHOLINERGIC RECEPTOR (Hm1)**

1. SUMMARY 32
2. INTRODUCTION 33
3. EXPERIMENTAL PROCEDURES 35
3.1 Materials 35
3.2 Epitope Tag and Expression of Hm1 36
3.3 Ligand Binding and Phosphatidyl Inositol Turnover Studies 37

3.4 Receptor Purification and Immunoprecipitation 37
4. RESULTS 40
4.1 Expression and Function of Epitope-Tagged Hm1 40
4.2 Solubilization of Epitope-Tagged and Untagged Hm1 40
4.3 Immunoprecipitation and Phosphorylation 41
5. DISCUSSION 42

**CHAPTER III. MUTATIONS IN THE CYTOPLASMIC LOOPS OF THE HUMAN m1 MUSCARINIC RECEPTOR INHIBIT INTERNALIZATION: CONFOCAL MICROSCOPY IN PERMEABILIZED AND SYNCHRONIZED CELLS**

1. SUMMARY 48
2. INTRODUCTION 49
3. EXPERIMENTAL PROCEDURES 51
3.1. Materials 51
3.2. Epitope-Tagged and Stable Expression of Hm1 51
3.3. Epitope-Tagged Mutants of Hm1 52
3.4. Receptor Binding, Internalization and Function 52
3.5 Laser Confocal Microscopy of EE-Hm1 Internalization 53
4. RESULTS 55
4.1 Expression and Function of Epitope-Tagged Hm1 55
4.2 Hm1 Internalization: Ligand Binding and Microscopy 56
4.3 Synchronized Internalization of EE-Hm1 58

5. DISCUSSION 59

5.1 Agonist-Induced Internalization 59

5.2 Synchronized Internalization 62

**CHAPTER IV MUTATIONAL ANSALYSIS OF THE THIRD CYTOPLASMIC LOOP DOMAINS IN G-PROTEIN COUPLING OF THE Hm1 MUSCARINIC RECEPTOR**

1. SUMMARY 73

2. INTRODUCTION 74

3. EXPERIMENTAL PROCEDURES 76

3.1 Materials 76

3.2 Construction and Expression of Hm1 and Mutants 76

3.3 Receptor Binding Assays and Data Analysis 76

3.4 Phosphatidyl Inositol Turnover 77

4. RESULTS 78

5. DISCUSSION 79

**REFERENCES** 8 6

## LIST OF TABLES

Chapter 1

Table I. Diprenorphine binding and forskolin-stimulated cAMP accumulation in cells expressing EE-μR and μR

Chapter 3

Table I. Binding and functional properties of Hm1 and epitope-tagged Hm1

Chapter 4

Table I. Inositol phosphate stimulation in deletion mutants of Hm1

## LIST OF FIGURES


| | |
|---|---|
| Figure 1.1 | Diprenorphine saturation binding curve for epitope-tagged μ opioid receptor |
| Figure 1.2 | Confocal Microscopy of epitope-tagged μ opioid receptor |
| Figure 1.3 | Immunoblot of epitope-tagged μ opioid receptor |
| Figure 1.4 | Phosphorylation of epitope-tagged μ opioid receptor |
| Figure 2.1 | Solubilization of epitope-tagged m1 muscarinic receptor |
| Figure 2.2 | Immunoprecipitation of epitope-tagged and untagged m1 muscarinic receptor |
| Figure 3.1(a-f) | Agonist-induced internalization of epitope-tagged m1 muscarinic receptor |
| Figure 3.2(a-f) | Agonist-induced internalization of EE-(d232-358) |
| Figure 3.3(a-b) | Deficient internalization of EE-(V127A/L131A) |
| Figure 3.4(a-f) | Synchronized Internalization of epitope-tagged m1 muscarinic receptor |
| Figure 4.1 | Amino acid sequence of the third intracellular loop of the m1 muscarinic receptor |
| Figure 4.2 | Dose-response curve for PI hydrolysis in Hm1-transfected cells. |

# INTRODUCTION

## OBJECTIVE

The overall objective of these experiments was to probe the mechanism of agonist-induced regulation of G protein-coupled receptors. Two cloned receptors, the rat μ-opioid receptor and the human m1 muscarinic cholinergic receptor, were used as model systems. Both are seven transmembrane domain receptors, predominantly expressed in the central nervous system. The specific aims of this research were to 1) develop a method to separate and identify the opioid and the muscarinic receptors when they are expressed in a human embryonic kidney cell line (HEK 293), 2) determine if agonist-induced phosphorylation is a regulatory mechanism for these receptors, 3) determine if agonist induces sequestration-internalization of these receptors by visualizing these processes in transfected cells, 4) identify by mutational analysis receptor domains in the muscarinic receptor which mediate receptor internalization and G-protein coupling.

## BACKGROUND

### G Protein-Coupled Receptors

More than eighty distinct receptors have been identified to date which couple to heterotrimeric G proteins (Birnbaumer et al., 1990). The starting point for our understanding of the structural and

mechanistic similarity of the members of this receptor family was the electron diffraction analysis of the light sensitive protein bacteriorhodopsin performed by Unwin *et al.* (Unwin and Henderson, 1975) and developed by Engelman *et al.* (Engelman et al., 1980). In 1982 the structure of the visual pigment, bovine rhodopsin, was predicted based on its amino acid sequence (Ovchinnikov et al., 1882). The similarity of this predicted structure, containing an extracellular amino terminus and seven hydrophobic membrane-spanning domains, to that demonstrated for bacteriorhodopsin was soon recognized. This structural paradigm was reinforced by the cloning of the human opsins (Nathans and Hogness, 1984) and the hamster β-adrenergic receptor (βAR) (Dixon et al., 1986), all of which contain a similar seven hydrophobic domain sequence. In the intervening years, the number of cloned transmembrane proteins predicted to share this structure has expanded rapidly. The published sequences for G protein-coupled receptors (GPCRs) include a wide range of sizes, varying from the 324 residue *mas* oncogene to the 744 residue thyroid-stimulating hormone receptor (Probst et al., 1992). The spectrum of ligands which bind to these receptors is also broad, and includes neurotransmitters, hormones, and neuropeptides, as well as light and odors. In the experiments described here, the μ-opioid receptor and the m1 subtype of the muscarinic cholinergic receptor have been chosen from the GPCR family as representative of neuropeptide and neurotransmitter receptors, respectively.

A number of GPCRs are prominent in the central nervous system. Because of the relatively slow onset and decay of their activity (relative to ion channels), GPCRs in the central nervous system have

been speculated to participate in responses to low concentrations of ligand, possibly at some distance from the transmitter release site (Hille, 1992). A very rapid time course of activity is generally not associated with the action of either endogenous opioid peptides or physiological concentrations of exogenous opioid drugs. Thus, this hypothetical model of GPCR function would seem appropriately applied to the recently cloned μ-opioid receptor (Chen et al., 1993, Fukuda et al., 1993, Thompson et al., 1993, Wang et al., 1993). The rat μ-opioid receptor contains 398 amino acids and is predicted to have seven transmembrane helices. The receptor is found in many areas of the central nervous system, including the striatum, thalamus and spinal cord (Thompson et al., 1993). Pharmacological description of the receptor prior to cloning indicated that the receptor is coupled via an inhibitory G protein to the adenylyl cyclase system. Recent work demonstrates that the receptor modulates both voltage-gated potassium and calcium channels (North et al., 1987, Schroeder et al., 1991, Wimpey and Chavkin, 1991), probably directly through the $G_{o\alpha}$ subunit of a G-protein (Brown and Birnbaumer, 1990, Nestler, 1992).

The m1 subtype of the muscarinic cholinergic receptor is found almost exclusively in the brain. The receptor was first cloned from porcine brain by Kubo *et al.* (Kubo et al., 1986), and since that time four additional subtypes (m2-5) have been cloned (Bonner et al., 1987, Bonner et al., 1988). The human m1 muscarinic receptor is 460 amino acids long, and is structurally remarkable for its large (156 amino acids) third intracellular loop (i3) between transmembrane domains five and six. The m1 receptor is coupled via $G_{q/11}$ to

phospholipase C, which cleaves phosphatidyl inositol 4,5-bisphosphate into diacylglycerol (DAG) and inositol triphosphate ($IP_3$). Release of $IP_3$ mobilizes intracellular calcium, which, in turn, activates $Ca^{2+}$/calmodulin-dependent protein kinase to phosphorylate intracellular substrates. When m1 is expressed in *Xenopus* ooctyes, the agonist-stimulated release of $IP_3$, and subsequent mobilization of $Ca^{2+}$, also evokes a chloride current (Fukuda et al., 1987). In addition, agonist binding to the the m1 receptor inhibits three types of currents, the N- and L-type $Ca^{2+}$ currents and the M-type $K^+$ current, via direct G protein-coupling to the ion channel. (Hille, 1992).

**Regulation of G Protein-Coupled Receptors**

The diminution of response following continuous exposure to a stimulus or agonist is defined as desensitization. Desensitization of the β-adrenergic receptor (βAR), the prototypic GPCR in studies of receptor regulation, has been shown to be implemented by several processes: serine-threonine phosphorylation, sequestration-internalization, binding to an arrestin protein, and downregulation. Phosphorylation of the βAR is believed to be responsible for short-term receptor desensitization. At least three kinases appear to act on the βAR: cAMP-dependent protein kinase (PKA), protein kinase C (PKC), and the β-adrenergic receptor kinase (βARK) (Hausdorff et al., 1990). The two isoforms of the βARK which have been identified are also referred to as GRK2 and GRK3 (G protein-coupled Receptor Kinase) in the current nomenclature to distinguish them from the second messenger kinases (Lefkowitz, 1993). Low concentrations (nanomolar) of agonist result in receptor phosphorylation at PKA

consensus sequences, while much higher agonist concentrations (micromolar range) result in phosphorylation by both kinases.

For the muscarinic receptor, agonist-induced phosphorylation has been reported for the m2 and m3 subtypes (Richardson and Hosey, 1992, Tobin and Nahorski, 1993). The m1 and m2 muscarinic receptors are phosphorylated by PKC *in vitro* (Haga et al., 1990, Richardson and Hosey, 1990), and the m2 subtype is a substrate for βARK (Kwatra et al., 1989). A muscarinic-specific GRK, the muscarinic acetylcholine receptor kinase (mAchR kinase), has also been identified which acts on both m1 and m2 receptors (Haga and Haga, 1992).

The μ-opioid receptor is phosphorylated *in vitro* by PKA (Harada et al., 1990), and the phosphorylated receptor is functionally uncoupled. The phosphorylation of the cloned opioid receptor (either μ or δ) has not been reported.

Receptor sequestration-internalization is a second mechanism proposed to effect receptor desensitization. Sequestration-internalization will be described simply as internalization since this latter process was the focus of the experiments described here. The βAR has been demonstrated to be internalized into cytoplasmic vesicles in response to agonist (Raposo et al., 1989, vonZastrow and Kobilka, 1994, vonZastrow and Kobilka, 1992). However the process is poorly understood. The mediators of GPCR internalization have not been identified, nor have the conditions been defined which stimulate internalization rather than phosphorylation of arrestin binding. Data on the pathway for internalization of the βAR as being clathrin-me-

diated or non-clathrin mediated, are conflicting (Raposo et al., 1989, vonZastrow and Kobilka, 1992).

Internalization of the muscarinic receptor has been extensively studied by ligand binding (Harden et al., 1985, Koenig and Edwardson, 1994), but morphological examination of muscarinic receptor internalization is limited (Raposo et al., 1987). Data for the role of internalization in opioid receptor desensitization is scant. Ligand binding studies of the endogenous receptor suggest that the δ–opioid receptor internalizes in response to agonist (Ornatowska and Glasel, 1992, vonZastrow et al., 1993), but the endogenous μ-opioid receptor does not appear to internalize in response to agonist (Cone et al., 1991). Thus GPCR desensitization is associated with a complex system of controls. Classification of the members of this large receptor family according to their regulatory mechanism is just beginning as each cloned receptor is examined in turn.

**Determinants of Receptor Coupling and Internalization**

The structural basis for coupling to G proteins and the principles which govern the G protein specificity of these receptors has not been defined for any GPCR. Investigations based on mutational analysis, peptide competition, and anti-receptor antibody interactions have suggested regions of the receptors which are essential to coupling. However, the possibility of multi-site determinants and the variation in intracellular domains across this large family, make simple sequence-to-function relations difficult to identify. The third cytoplasmic domain of the GPCRs was assumed to be the site of the coupling determinant, but recent experiments suggest that other cy-

toplasmic domains may contribute to or determine coupling (Moro et al., 1993, Moro et al., 1994, Wong and Ross, 1994).

Receptor desensitization appears to be related to interaction with cytoplasmic mediators, including kinases, adaptors and arrestin-like proteins. Elucidation of the GPCR domains which interact with these mediators has begun for the βAR, but is much more complete for single transmembrane spanning receptors such as the transferrin, low density lipoprotein, polymeric immunoglobulin, and mannose 6-phosphate receptors (reviewed in Trowbridge, 1991). For the GPCRs, sites in both the i2 and i3 loops of the muscarinic receptor have been identified as contributors to agonist-mediated internalization (Maeda et al., 1990, Moro et al., 1994). As is the case for G protein-coupling determinants, identifying a single domain responsible for receptor desensitization may be ill-conceived. It is also likely that the different mediators of desensitization act in succession on their receptor targets, thereby achieving a fine-tuning of the receptor population available for activation (vonZastrow and Kobilka, 1994). In conclusion, the search for the domains responsible for regulation of the GPCRs presents a new challenge in deciphering protein signals, since the regulatory determinants, like the coupling determinants, may be separated from one another in both time and in space.

# CHAPTER 1

# EPITOPE-TAGGED μ-OPIOID RECEPTOR EXPRESSED IN HEK 293 CELLS:

## CONFOCAL MICROSCOPY, IMMUNOPRECIPITATION AND PHOSPHORYLATION


## SUMMARY

We have expressed the cloned μ-opioid receptor (Chen et al., 1993) in high abundance (5.5 x $10^6$ sites/cell) with an amino-terminal epitope tag (EYMPME) in HEK 293 cells. The epitope-tagged receptor (EE-μR) was similar to the untagged receptor (μR) in binding, and more potent than untagged receptor in agonist-dependent inhibition of cAMP accumulation (IC50 for morphine 2.1 ± 0.3 nM and 20 ± 8 nM, respectively) and maximum inhibition of cAMP (μR: 83% and EE-μR: 76%). There was no evidence of downregulation of the EE-μR by ligand binding during a 19 h exposure to 10 μM morphine. By confocal microscopy, labeled receptor remained largely confined to the plasma membrane during the 19 h morphine exposure. EE-μR can be solublized in detergent (CHAPS) and immunoprecipitated by an anti-epitope monoclonal antibody in a diprenorphine-bound con-

formation. Immunoblotting revealed a prominent band at ~70 kD with weaker bands at ~65 kD. Immunoprecipitation of phosphorylated EE-μR showed a prominent signal at 65-70 kD, regardless of exposure to 10 μM morphine. Thus the μ-opioid receptor in HEK 293 cells is strongly coupled to adenylyl cyclase and fails to desensitize or internalize. Unlike other G protein-coupled receptors, it undergoes phosphorylation largely independent of agonist stimulation.

## INTRODUCTION

The μ-opioid receptor recognizes morphine and other opioid drugs as well as endogenous peptides such as β-endorphin. Pharmacologic effects generally associated with the μ-subtype of opioid receptor include analgesia, respiratory and circulatory depression, and, importantly, opioid tolerance and dependence. The cloned μ-receptor (Chen et al., 1993, Thompson et al., 1993, Wang et al., 1993) is a seven transmembrane-spanning receptor and is a member of the family of G-protein coupled receptors (GPCRs). The μ-opioid receptor is functionally coupled to several effector pathways including modulation of $K^+$ and $Ca^{2+}$ channels (North et al., 1987, Schroeder et al., 1991, Wimpey and Chavkin, 1991), and the inhibition of adenylyl cyclase (Carter and Medzihradsky, 1993, Sharma et al., 1975).

Opioid tolerance, in which repeated exposure to an opioid results in reduced effect, is a major therapeutic problem, particularly in the treatment of chronic pain. Tolerance has been intensively in-

vestigated, but remains poorly understood (reviewed in (Nestler, 1992). There is no consistent relationship between opioid tolerance and receptor number, affinity or coupling efficiency (Loh and Smith, 1990). Thus the establishment of tolerance appears to be complex, with adaptations at multiple levels of signal transduction and integration. While tolerance is complex, desensitization, the diminution of a stimulated response following continuous exposure of a receptor to agonist, may contribute to tolerance and can be examined more readily. The desensitization of the $\beta_2$-adrenergic receptor ($\beta_2$AR) has been extensively characterized (reviewed in (Hausdorff et al., 1990)). Two processes are temporally associated with $\beta_2$AR desensitization: 1) stimulus-dependent phosphorylation and subsequent binding of regulatory proteins (e.g., β-arrestin) to the receptor (Hausdorff et al., 1989, Lohse et al., 1990) and 2) receptor internalization-sequestration (vonZastrow and Kobilka, 1994, vonZastrow and Kobilka, 1992, Yu et al., 1993).

To study the molecular and cellular mechanisms underlying tolerance to opioid action, we examined the processes associated with receptor desensitization. Neither the phosphorylation nor the intracellular distribution of the cloned μ-opioid receptor have been described previously. We first added an epitope to the amino terminus of the μ opioid receptor (μR), and found no significant differences between the biochemical characteristics of epitope-tagged and untagged receptors. We then used the corresponding monoclonal antibody to immunoprecipitate the phosphorylated epitope-tagged receptor and to localize it by immunofluoresence confocal microscopy. Immunocytochemical and ligand binding studies indicate that even

prolonged agonist exposure does not result in receptor redistribution or internalization. In addition, the epitope-tagged μ-opioid receptor is phosphorylated in the basal state, and brief exposure to agonist results in only a small increase in receptor phosphorylation. Our data suggest that the intracellular trafficking and phosphorylation of the μ-opioid receptor in response to agonist are distinct from those known to control other G-protein coupled receptors.

## EXPERIMENTAL PROCEDURES

### Materials.

The rat μ-opioid receptor cDNA was provided by Lei Yu (Indiana University School of Medicine). [$^3$H]-diprenorphine (FW = 407, specific activity 47 Ci/mmol) was obtained from the National Institute of Drug Abuse (Rockville, MD). Morphine sulfate was from Merck Inc. Fish gelatin, poly-L-lysine, saponin, CHAPS were purchased from Sigma Chemical Co (St. Louis, MO), and Fluoromount G from Fisher Scientific (Pittsburgh, PA). All other reagents were of analytical grade quality from common commercial sources. Restriction enzymes were from Boehringer Mannheim or Bethesda Research Laboratories.

Monoclonal antibodies to the epitope EYMPME (Grussenmeyer et al., 1985) were purchased from Onyx Inc. (Richmond, CA). FITC-conjugated anti-mouse IgG antibodies were purchased from Cappell Technika (Durham, North Carolina). For Western blotting, PVDF membrane was from Millipore Corp. (Bedford, MA), and alkaline

phosphatase conjugated rabbit anti-mouse IgG and development reagents were from BioRad (Hercules, CA).

**Epitope-tagged μ-opioid receptor (EE-μR)**

The sequence TTTTAAGCTTACCATGGAATACATGCCAATGGAA GACAGCAGCACCGGCCCAGGG containing a *HindIII* restriction site, the start codon, and a sequence encoding the epitope EYMPME (underlined), served as the 5' primer in order to append the epitope tag to the amino-terminal of the rat μ-opioid receptor by the polymerase chain reaction. The 3' primer sequence (GCTCTAGAGCGAGG GTCTGGATGGTG) contained a stop codon and an *XbaI* restriction site. The amplified fragment (EE-μR) was ligated into pRc/CMV (Invitrogen, San Diego, CA) which contains a neomycin-resistance gene, and subcloned into the *E. coli* TOP 1OF' strain. The 5' sequence containing the epitope was verified by automated sequencing. Human embryonic kidney cells (HEK 293) were transfected by the calcium phosphate method, and clonal cell lines stably expressing EE-μR were selected with 400 μg/ml G-418 and maintained in DMEM/H-16/F-12 with 10% FCS and 200 μg/ml G-418.

**Ligand Binding Assays and cAMP Assay**

EE-μR expression was quantitated with [$^3$H]-diprenorphine. HEK 293 cells stably expressing EE-μR were harvested into PBS, and triplicate samples were incubated with 10 nM [$^3$H]-diprenorphine and differing concentrations of diprenorphine or morphine sulfate in

50 mM Tris, pH 7.4. Cells were incubated for 2 hours at 20°C and harvested on GF/C glass filters which were washed three times with cold PBS, and $^3H$ content determined. Displacement data were fit to the logistic function, $B = B_{max} - [B_{min} * L]/ [IC50 + L] + NSB$, where B is the tracer bound, L = diprenorphine or morphine concentration, and NSB is the nonspecific binding. Protein content was determined by the method of Bradford (Bradford, 1976).

Agonist-induced downregulation (i.e., internalization with subsequent lysosomal degradation) of EE-μR was evaluated by measuring the change in binding of the lipophilic opioid ligand [$^3H$]-diprenorphine in whole cells following exposure to 10 μM morphine sulfate. Stably transfected cells were seeded at 2 x $10^6$/ml on six-well plates and incubated at 37°C in complete medium throughout. Triplicate wells were treated for 0, 1, 1.6, 4, 14, and 20 hrs with 10 μM morphine. Cells were washed 4 times with complete medium and once with 50 mM Tris (pH 7.4), 0.2% BSA, and labeled in the same buffer with 10 nM [$^3H$]-diprenorphine for 90 minutes at room temperature. Cell were harvested by scraping and collected on GF/C filters which were washed three times with cold PBS and counted.

Inhibition of forskolin-induced cAMP accumulation by morphine was determined in stably transfected cells by radioimmunoassay (Amersham, Arlington Heights, IL). Data are expressed as percent inhibition of forskolin-stimulated cAMP accumulation.

Statistical comparison of values for epitope-tagged and untagged receptor was performed by two-tailed t-test using a pooled-variance estimate and a level of significance of $p < 0.05$ (Glantz, 1981; Zar, 1974).

## Laser Confocal Microscopy

Cells were prepared for microscopy as described by Wong et al. (Wong and Brodsky, 1992). Cells stably expressing the EE-μR were grown overnight at low density in complete medium on chamber slides (Nunc Inc., Napperville, IL) pretreated with poly-L-lysine. Cells were exposed to 10 μM morphine sulfate for different periods of time at 37°C in 5% $CO_2$/95% air. The medium was removed and cells were washed in PBS and fixed with 3.7% paraformaldehyde in PBS for 10 minutes. Cells were permeabilized with 0.04% saponin, 0.25% cold water fish gelatin in PBS (IMF buffer) for 10 minutes at room temperature, and then treated for 1 hour with a 1:1000 dilution of anti-EE mAb in IMF buffer. After 3 washes with the buffer, cells were treated with a 1:3000 dilution of FITC-conjugated rabbit anti-mouse IgG for 30 minutes. Cells were washed 3 times in IMF buffer and once in water, dried and mounted, and stored at 4°C.

Cells were visualized using a krypton-argon laser coupled with a BioRad MRC-600 confocal head attached to a Optiphot II Nikon microscope with a Plan Apo 60X 1.4 NA objective lens. Samples were scanned for FITC emission using a blue high sensitivity (BHS) filter block. Collection parameters were 5 s/scan, 5 frames/image, Kalman filter, motor step size 0.7 μm, diaphragm one-third open. Optical sections along the z-axis of isolated cells were stored on 940 MB optical disc (Panasonic Inc). Images from the central plane of the cell were compared to assess internalization/sequestration.

**Receptor Purification and Immunoprecipitation**

Confluent flasks with ~2 x $10^7$ HEK 293 cells stably expressing EE-μR were washed briefly with PBS and incubated with lysis buffer (5 mM Tris, pH 7.4, 2 mM EDTA, 1 mM EGTA, 1 mM benzamidine, 1 μg/ml leupeptin, 1 μg/ml aprotinin, 10 μM morphine sulfate) for 10 minutes on ice. All succeeding steps were performed at 4°C unless otherwise noted. Cells were scraped into a Dounce homogenizer and the ruptured cells were centrifuged at 1000 x g for 10 minutes. The supernatant was centrifuged at 30,000 x g for 30 minutes. For immunoblotting, the protein content of the washed membrane pellets was determined by Bradford assay (BioRad, Hercules, CA), and the protein content of pellets was equalized by resuspending in SDS sample buffer. Following separation by 8% PAGE, proteins were transferred to a PVDF membrane (Millipore, Bedford, MA) for 2 hour in Tris-glycine buffer. Membranes were blocked (3% instant milk in Tris-buffered saline, 0.05% Tween-20), and incubated with a 1:100 dilution of anti-epitope antibody (anti-EE mAb) for 2 hours at 25°C. Washed membranes were visualized by incubation with 1:2000 dilution of alkaline phosphatase-coupled anti-mouse antibody followed by reaction with chromogenic substrates.

Solubilization of the EE-μR used the detergent CHAPS as described previously for the opioid receptor (Cote et al., 1993, Ofri et al., 1992). Pelleted membranes were first incubated with 10 nM [$^3$H]-diprenorphine for 1 hour at 4°C, resuspended in a buffer consisting of 50 mM Tris (pH 7.4), 100 mM NaCl, 2 mM EDTA, 1 mM EGTA, 10 mM CHAPS, 1 mM benzamidine, 1 μg/ml leupeptin, 1 μg/ml aprotinin. The solution was incubated for 40 minutes at 4°C with

gentle mixing. The solubilization reaction mixture was centrifuged at 105,000 x g for 40 minutes at 4°C and the supernatant was applied to a Sephadex G-50 gel filtration column pre-equilibrated with 50 mM Tris, 2mM CHAPS. Fractions were collected and the $^{3}H$ content of 100 µl aliquots was determined in 5 ml Scintiverse II (Fisher Biotech, Pittsburgh, PA).

For immunoprecipitation, membrane pellets were first resuspended in Tris-NaCl buffer including protease inhibitors as described, and incubated in 10 nM diprenorphine, 140 pM [$^{3}H$]-diprenorphine for one hour at 4°C. Membranes were centrifuged at 30,000 x g for 20 minutes, the pellet was resuspended in Tris-NaCl buffer, and CHAPS was added to a final concentration of 10 mM. The solubilization reaction was gently mixed for 30 minutes and centrifuged at 105,000 x g for 40 minutes. The supernatant, containing CHAPS-solubilized membrane, was incubated with a 1:40 dilution of anti-EE mAb and 50 µl of a 33% slurry of washed protein G sepharose 4 fast flow for 12 hr. Beads were washed in cold Tris-NaCl buffer without CHAPS and were harvested on GF/C filters pretreated with 0.3% polyethyleneimine. Filters were washed three times with ice-cold PBS and counted.

**Immunoprecipitation of the Phosphorylated EE-µR**

Phosphorylation of EE-µR was performed in permeabilized cells by a modification of the procedure described by Raymond (Raymond, 1991). Confluent T-75 flasks containing 2 x $10^{7}$ EE-µR expressing cells were washed once gently and incubated for 15 minutes at 37°C

in phosphate-free medium. After harvesting and brief centifugation cell pellets were resuspended in Tris-NaCl buffer (50 mM Tris, pH 7.4, 100mM NaCl, 10mM sodium pyrophosphate, 10 mM NaF 1 mM benzamidine, 1 μg/ml leupeptin, 1 μg/ml aprotinin) and aliquots of digitonin (Wako BioProducts, Richmond VA) were added until ~90% of cells were permeabilized as defined by failure to exclude trypan blue dye. Final digitonin concentration was 150-200 μM. Cells were treated with 10 μM morphine sulfate or buffer and 1 μCi/μl [$\gamma$-$^{32}$P]-ATP (7000 Ci/mmol, Dupont/NEN, Boston, MA) for 15 minutes at 25°C with gentle rocking. Labeled cells were washed twice with Tris-NaCl buffer, homogenized in a Dounce homogenizer, and centrifuged at 1000 x g for 10 minutes. The supernatant was centifuged at 30,000 x g for 30 minutes, and the resulting membrane pellet was then solubilized in CHAPS and immunoprecipitated as described above. The incorporation of $^{32}$P into the 105,000 x g supernatant was determined at the time of immunoprecipitation to equalize control and transfected samples. SDS-PAGE gels were autoradiographed and bands were quantitated by scanning densitometry.

## RESULTS

### Stable expression of μ and EE-μ opioid receptor

HEK 293 cells, which do not express endogenous opioid receptor, were cotransfected with the μ-opioid (μR) or the EE-μ opioid (EE-μR) receptor and a geneticin resistance gene. Receptor expression was assessed by [$^3$H]-diprenorphine binding. Of six EE-μR clones se-

lected for geneticin resistance, one clone expressed 5.5 x $10^6$ EE-μR sites per cell by [$^3$H]-diprenorphine binding and was further analyzed (Table I). The μR was expressed in twelve clones which were resistant to geneticin, and one clone which expressed 4.0 x $10^6$ sites/cell was selected for this study. In a [$^3$H]-diprenorphine saturation binding experiment in intact cells expressing the EE-μR, the $K_d$ was 3.2 ± 0.9 nM ($B_{max}$, 43.6 ± 5.3 pmole/mg protein, Figure 1.1), and for displacement by morphine the IC50 was 558 ± 148 nM. In cells expressing μR, the $K_d$ for diprenorphine was 2.4 ± 0.5 nM ($B_{max}$, 34.6 ± 4.0 pmole/mg protein) and the IC50 for morphine was 667 ± 110 nM (Table I).

The functional coupling of EE-μR was determined by measuring the forskolin-stimulated accumulation of cAMP in the presence of morphine. The IC50 for morphine was 2.1 ± 0.3 nM (Table I). In HEK cells stably transfected with μR, the IC50 was 20 ± 7.7 nM. In the presence of 1 μM morphine, cAMP accumulation was inhibited by 83% in EE-μR cells and 76% in cells with a similar level of expression of μR. Naloxone (10 μM) reversed this inhibition to 26% and 47% of control stimulation in cells expressing epitope-tagged and untagged receptor, respectively. Pretreatment of μR transfected cells with morphine (300 nM for 12 hours) did not decrease, and in fact may enhance, the maximum inhibition of cAMP accumulation by 10 μM morphine (μR:. 76%, treated vs. 66% untreated).

**Confocal Laser Microscopy of EE-μ opioid receptor**

The epitope tagged μ-opioid receptor was visualized as a strong fluorescent signal which localized to the plasma membrane in untreated EE-μR cells. Chamber slide grown EE-μR cells were exposed to 10 μM morphine at 37°C for 20 minutes, 2, 4, 14, and 24 hours and subsequently examined by immunofluorescence confocal microscopy. Prior to morphine exposure, the opioid receptor was visible as an intense signal at the plasma membrane (Figure. 1.2a). Very few cytoplasmic vesicles containing the opioid receptor were visible. The receptor remained confined to the plasma membrane without visible membrane redistribution or internalization into cytoplasmic vesicles following treatment with 10 μM morphine. Sequential confocal micrographs demonstrated that the EE-μR persisted at the cell membrane without evidence of internalization during the 19 hr exposure to maximally stimulating concentrations of morphine (Fig. 1.2b-d).

Measurement of ligand binding was performed to determine if receptor downregulation contributes to agonist-induced regulation of the μ-opioid receptor. There was no detectable loss of binding to the lipophilic ligand [$^3$H]-diprenorphine following treatment with 10 μM morphine for different periods of time up to 19 hours (557 ± 91 fmoles at time 0; 447 ± 88 fmoles at 19 h). These data indicate that there was no detectable downregulation of the EE-μ opioid receptor over the time-course examined immunohistochemically.

**Purification of the EE-μ opioid receptor**

To determine if the epitope-tagged μ-opioid receptor could be solubilized in detergent with retention of bound diprenorphine, membranes from cells expressing EE-μR were labeled with [$^3$H]-diprenorphine, washed and solubilized in 10 mM CHAPS. Gel filtration chromatography of high speed supernatants yielded two distinct peaks of [$^3$H]-diprenorphine activity. Early fractions, corresponding to detergent-solubilized EE-μR with bound ligand, were separated from low molecular weight free ligand (data not shown).

To determine if solubilized receptor could be immunoprecipitated, [$^3$H]-diprenorphine-bound membranes were solubilized in 10 mM CHAPS and immunoprecipitated with anti-EE mAb and protein G sepharose beads. After filtration and washing, 62% of the solubilized [$^3$H]-diprenorphine activity was retained on glass filters. Only a negligible amount of [$^3$H]-diprenorphine was immunoprecipitated and retained on glass filters from untransfected HEK 293 cells.

To identify the tagged opioid receptor on SDS-PAGE, washed membranes from EE-μR–expressing cells were solubilized in Laemmli sample buffer and separated on an 8% SDS-PAGE gel. Immunoblotting with anti-EE mAb followed by chromogenic detection revealed a prominent band at ~70 kD and weaker bands at ~65 kD (Figure 1.3, lane A). No corresponding bands were visible in membranes containing an equal amount of protein from untransfected HEK 293 cells (Figure 1.3, lane B).

**Phosphorylation of the EE-μ opioid receptor**

Immunoprecipitation of the EE-μ receptor following a 15 minutes pulse of [$\gamma$-$^{32}$P]-ATP in digitonin-permeabilized cells revealed that the μ-opioid receptor was phosphorylated both in cells treated for 15 minutes with 10 μM morphine sulfate (Figure 1.4, lane A) and in cells not exposed to agonist (Figure 1.4, lane B). Scanning densitometry of 65-70 kD bands showed only a small increase in intensity of the $^{32}$P signals with the ratio of treated to untreated cells equal to 1.78 ± 0.7 (mean of three experiments). Thus, agonist exposure had only a moderate effect on phosphorylation of the tagged opioid receptor when compared to the high level of phosphorylation in the unstimulated receptor.

## DISCUSSION

We have stably expressed an amino-terminal epitope-tagged rat μ-opioid receptor (EE-μR) in HEK 293 cells and compared it to wild-type receptor (μR) in ligand binding and functional assays. The EE-μR is expressed in high abundance (5.5 x $10^6$ sites/cell) in stably transfected human cells. The high level of expression facilitates characterization of opioid receptor regulation and will permit isolation of intracellular mediators of opioid receptor function. While binding studies of the EE-μR indicate high levels of expression, the affinity for opioid ligands of the EE-μR and μR in this system is approximately 10 fold lower than has been observed for the cloned receptor. The IC50 for morphine displacement of diprenorphine in

membranes of transfected cells is ~50 nM (Lei Yu, personal communicatio

n). Several factors could contribute to this discrepancy. First, we have characterized ligand binding in whole cells, rather than in cell membranes (Chen et al., 1993, Thompson et al., 1993, Wang et al., 1993). Our data are consistent with previous reports of a 35-fold decrease in μ-opioid receptor affinity for morphine in intact cells compared to cell membranes (Toll, 1992). Second, published results for the binding of the transfected μ-opioid receptor (Chen et al., 1993, Raynor et al., 1994) were performed in transiently, rather than stably, transfected cells of different cell lines from that presented here. Third, EE-μR is expressed in very high abundance in our stable expression system, with 30-times as many receptors as typically observed for the native μ-opioid receptor (Yu et al., 1986). This level of expression may affect the affinity state for the receptor, though receptor number generally affects binding maximum and $K_d$. The observed diprenorphine affinity does not appear to be affected by the epitope itself, since we found similar binding affinities for diprenorphine when an untagged rat μ-opioid receptor was stably expressed in HEK 293 cells.

Agonist stimulation of the μ-opioid receptor results in inhibition of the forskolin-induced release of cAMP. The IC50 for inhibition of cAMP accumulation by the endogenous opioid receptor in differentiated human neuroblastoma (SH-SY5Y) cells is 30-50 nM (Yu and Sadee, 1988), which is similar to the value observed for μR-transfected cells (20 nM ± 7.7, Table I). In EE-μR expressing cells, morphine is ten times more potent in inhibiting cAMP accumulation

with an IC50 of 2.1 ± 0.3 nM. The increase in morphine potency at the EE-μR may also be reflected by the diminished ability of 10 μM naloxone to reverse this inhibition (26% control) when compared to reversal effected in μR-transfected cells (47% control). The maximum inhibition of cAMP accumulation by morphine in EE-μR transfected cells is also higher (83% inhibition) than that observed for endogenous receptor (70%) (Yu et al., 1990), indicating that the highly-expressed EE-μR is fully functional. This result also contrasts to the rather low level of cAMP inhibition (18%) in previous studies with transiently transfected μR cDNA (Chen et al., 1993).

Agonist-induced receptor downregulation (internalization with lysosomal degradation) has been proposed as mechanisms for adrenergic receptor desensitization (Yu et al., 1993). In contrast, previous data for the endogenous opioid receptor indicate there is little agonist-induced internalization or downregulation in SH-SY5Y cells (Yu and Sadee, 1988) or in SK-N-SH cells, which express predominantly μ-type opioid receptor (Cone et al., 1991). However, recent studies revealed some downregulation to occur in SK-N-SH cells expressing both μ- and δ-opioid receptors (Baumhaker et al., 1993). We found no evidence for agonist-induced downregulation of the EE-μR in [3H]-diprenorphine binding studies following exposure to high concentrations (10 mM) of morphine for up to 19 hours.

The immunocytochemistry and subcellular localization of the cloned μ-opioid receptor has not been examined previously. Earlier studies {Gramsch, 1988 #60, Hassan et al., 1989) with monoclonal anti-idiotype antibodies in NG108-15 cells found δ-opioid receptor immunoreactivity primarily at the plasma membrane, and some cy-

toplasmic clusters of receptor were observed in one study (Ornatowska and Glasel, 1992). The effect of agonists on subcellular localization was not examined in previous studies. In the present study, on optical sections through the cell, the EE-μR was clearly visualized at the plasma membrane. The receptor remained confined to the plasma membrane with minimal agonist-induced internalization following exposure to 10 μM morphine for as long as 19 hrs. The subcellular localization of the EE-μR on confocal microscopy is consistent with the lack of receptor downregulation found in ligand binding studies, since internalization precedes lysosomal targeting. Thus intracellular receptor trafficking does not appear to contribute substantially to the early regulation of μ-opioid receptor activity. Failure to internalize in response to agonist has also been reported for the $M\alpha_{2H\text{-}10}$ adrenergic receptor subtype (vonZastrow et al., 1993). In contrast, morphologic studies indicate that other G-protein coupled receptors such as the $\beta_2$-adrenergic receptor (vonZastrow and Kobilka, 1994, vonZastrow and Kobilka, 1992), the $M\alpha_{2\text{-}4H}$ receptor (vonZastrow et al., 1993), and the m1 muscarinic receptor (Arden, manuscript in preparation) undergo agonist-induced internalization-sequestration in transfected HEK cells. For both the adrenergic and muscarinic receptors, endocytosis of the receptor is observed within the first minutes following agonist exposure, and vesicles containing receptor continue to accumulate for longer periods. Thus, GPCRs are differentially regulated by subtype-specific trafficking mechanisms, and in the case of the μ-opioid receptor, internalization cannot be demonstrated during the first hours following agonist exposure.

We present here the first immunoblot analysis of the cloned μ-opioid receptor, identified via a synthetic epitope on the amino terminus. The receptor is a ~70 kD protein on SDS-PAGE of crude membrane preparations from transfected HEK 293 cells. The relative molecular mass of ~70 kD is higher than expected based on the 398 residue amino acid sequence alone. Weaker bands at ~65 kD suggest that the ~70 kD receptor may be glycosylated since the μR contains multiple potential glycosylation sites (five asparagines) at the amino terminal (Chen et al., 1993). A purified μ-opioid receptor has also been shown previously to be a substrate for endoglycosidase F by Eppler et al. (Eppler et al., 1993). The immunoblot of the EE-μR provides a standard for positively identifying the receptor following separation by immunoprecipitation and subcellular fractionation, and will enable more detailed analyses of the biochemistry and cell biology of this receptor.

We have documented that the tagged μ-opioid receptor is phosphorylated in the basal state, and that brief exposure (15 minutes) to concentrations of agonist >1000-times the EC50 results in only a small increase in the level of phosphorylation. By comparison, phosphorylation of the m3 muscarinic receptor is 10-times greater than control following a 15 minute exposure to agonist (Tobin and Nahorski, 1993). The μ-opioid receptor was shown to be phosphorylated by cAMP-dependent protein kinase in reconstituted receptor preparations from rat brain (Harada et al., 1990). In reconstituted vesicles phosphorylation of the μ−opioid receptor by cAMP-dependent protein kinase functionally uncouples the receptor from $G_i1$ (Harada et al., 1989). Taken together, these data suggest that phos-

phorylation does regulate the μ-opioid receptor, but that the kinetics of phosphorylation appear to be different from those of other GPCRs. The continuous phosphorylation of the μ-opioid receptor may play an important role in regulating the receptor and controlling its physiological function.

In conclusion, we have developed a system to rapidly purify a transfected μ-opioid receptor and have probed the mechanism of opioid receptor regulation. It will be of interest, and potentially of therapeutic importance, to clarify the mechanism of μ-opioid receptor modulation, particularly the role of phosphorylation, since the regulation of this receptor appears to differ from that of other GPCRs examined to date.

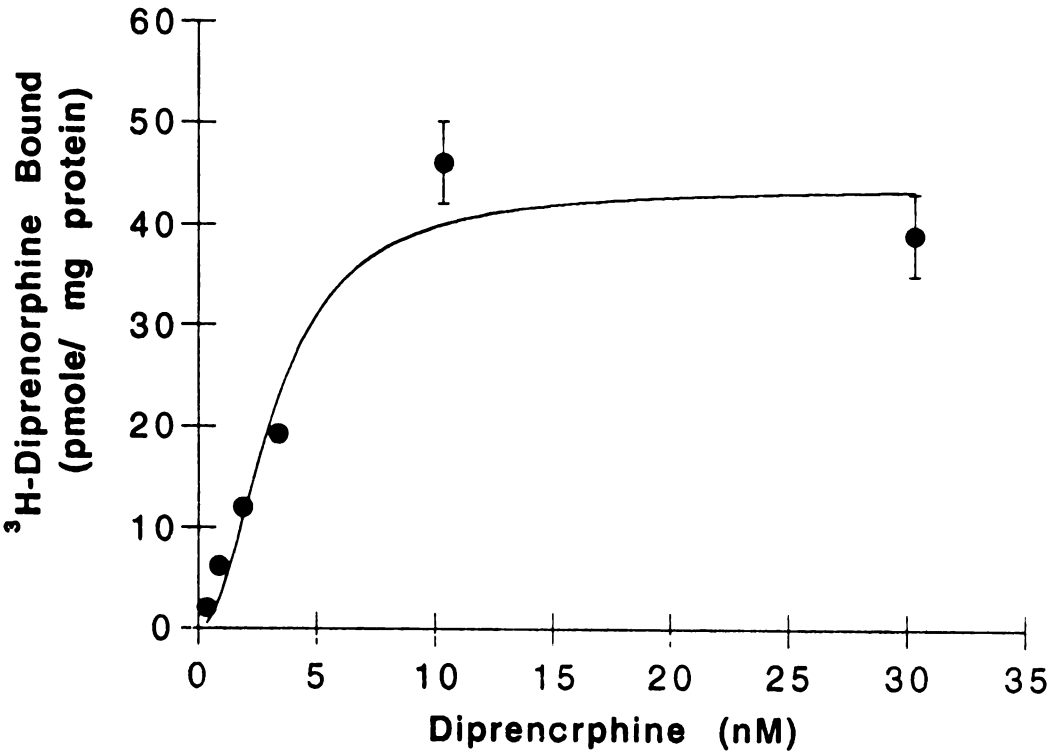


Figure 1.1. Diprenorphine saturation binding curve for epitope-tagged μ-opioid receptor transfected HEK 293 cells. Washed cells were incubated at 25°C for 2 hours with 10 nM [$^3$H]-diprenorphine and different concentrations of unlabelled diprenorphine, and the resultant saturation curve was plotted. $K_d$ was 3.4 ± 0.8 nM and $B_{max}$ was 3.4 ± 0.4 pmole/mg protein.

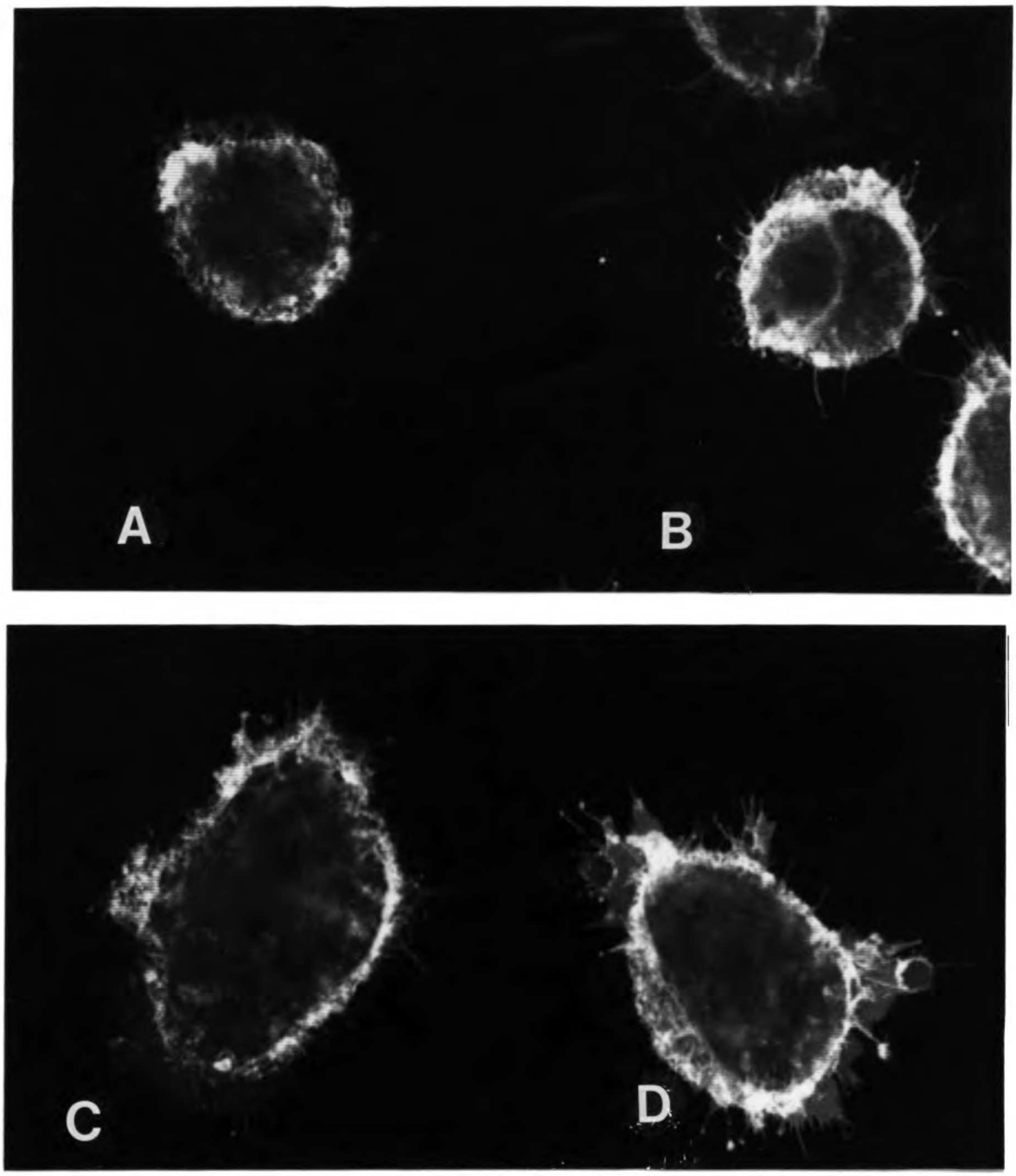


Figure 1.2. Confocal microscopy of epitope-tagged μ-opioid receptor treated with morphine. Untreated cells (A); Cells treated with 10 μM morphine for 2 h (B); 4 h (C); and19 h (D). Few intracellular vesicles which stained for EE-μR were observed with or without agonist exposure (compare to Figure 3.1(a-f) for EE-Hm1).

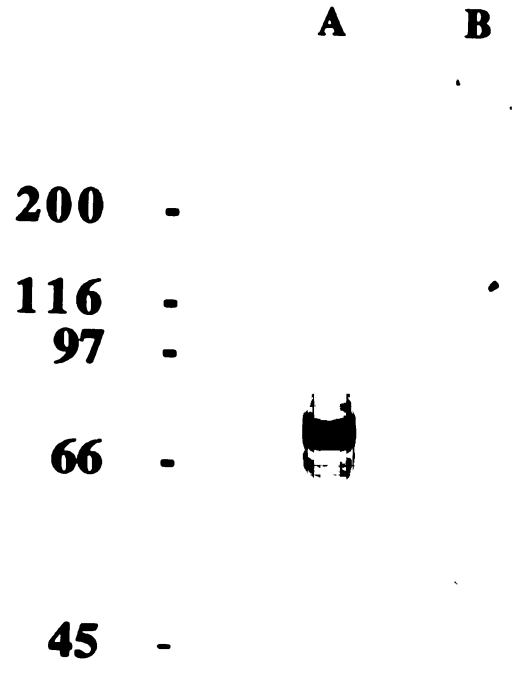


Figure 1.3. Immunoblot of epitope-tagged μ-opioid receptor. EE-μR transfected cells were homogenized and membranes were solubilized, separated on 8% SDS-PAGE, and blotted with anti-EE monoclonal antibody. Lane A, EE-μR expressing cell membrane; lane B, untransfected HEK 293 cell membrane; molecular weight markers as shown.

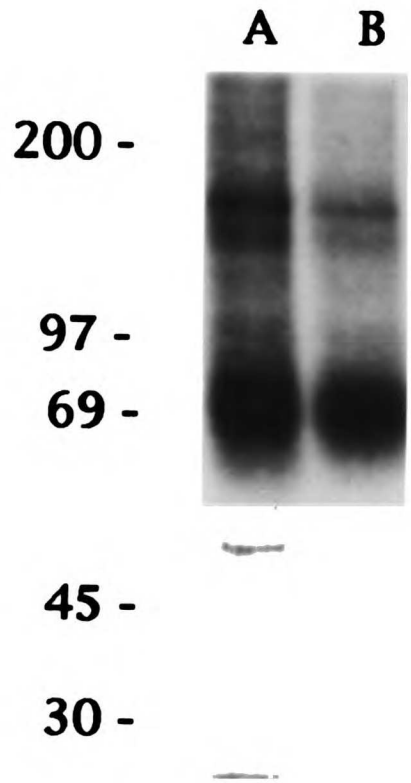


Figure 1.4. Phosphorylation of the epitope tagged μ-opioid receptor. HEK 293 cells stably expressing EE-μR were permeabilized with digitonin and labeled with [$\gamma$-$^{32}$P]-ATP, immunoprecipitated with anti-EE mAb, and separated on 8% reducing SDS-PAGE. Lane A, EE-μR expressing cells treated with 10 μM morphine sulfate for 15 minutes; Lane B, untreated EE-μR expressing cells; molecular weight standards as shown. The data are representative of three experiments performed. Exposure time 40 hours at -80°C.

TABLE 1. Diprenorphine binding and forskolin-stimulated cAMP accumulation in HEK 293 cells expressing EE-μR and μ-R. Values are expressed as mean ± SD. Signifcance differences were defined by values of $p < .05$ and indicated by an asterisk (*).

| | EE-μR | μR |
|---|---|---|
| **Sites/cell** | 5.5 X $10^6$ | 4.0 X $10^6$ |
| **Diprenorphine saturation** | | |
| **$K_d$ (nM)** | 3.2 ± 0.9 | 2.4 ± 0.5 |
| **$B_{max}$ (pmole/mg protein)** | 43.8 ± 5.3 | 34.6 ± 4.0 |
| **Diprenorphine displacement** | | |
| **Morphine IC50 (nM)** | 558 ± 148 | 667 ± 110 |
| **Morphine Inhibition of cAMP Accumulation** | | |
| **$E_{max}$ (% Inhibition)** | 83 | 76 |
| **EC50 (nM)** | | |
| **(-) Morphine Pretreatment** | 2.1 ± 0.3* | 20 ± 7.7* |
| **(+) Morphine Pretreatment** | NA | 25 ± 14 |

# CHAPTER 2

# PURIFICATION AND IMMUNOPRECIPITATION OF EPITOPE-TAGGED HUMAN m1 MUSCARINIC CHOLINERGIC RECEPTOR

## SUMMARY

The human m1 muscarinic receptor was modified by the addition of a synthetic epitope (EYMPME) to the amino terminus and stably expressed (~4 x $10^5$ sites/cell) in HEK 293 cells. The epitope-tagged receptor (EE-Hm1) was similar to the wild-type receptor in maximal ligand binding and inositol phosphate hydrolysis. The Hm1 was solubilized to a limited extent (~17% of total receptor expression) in digitonin/cholate, and could be specifically immunoprecipitated with its bound hydrophilic antagonist ([$^3$H]-NMS) by an anti-epitope monoclonal antibody. Immunopreciptates from Hm1 expressing cells which were permeabilized and labelled with [$\gamma$-$^{32}$P]-ATP showed a low level of basal phosphorylation with no evidence of agonist-mediated phosphorylation. We conclude that the epitope-tagged Hm1 receptor can serve as a fully-functional model of the wild-type Hm1 receptor, which can be immunoprecipitated in a soluble form, and that the epitope-tagged receptor is phosphorylated in unstimulated cells. These results suggest that rapid agonist-induced phosphorylation may not be a regulatory mechanism for Hm1.

## INTRODUCTION

The family of seven transmembrane domain (7 TMD) receptors includes a spectrum of neurotransmitter and neuropeptide receptors, ranging from the muscarinic cholinergic and metabotropic glutamate receptors to the substance P and VIP receptors (reviewed in Lameh et al., 1990). The prototypic receptor of this family is the β-adrenergic receptor whose structure, effector pathways, and regulation have been studied intensively.

Desensitization, the diminution of a response during the continuous exposure to a stimulus or an agonist, is a critical mechanism in the modulation of neurotransmission at the neuronal level. For the prototypic 7 TMD β-adrenergic receptor (βAR), desensitization has been associated with three cellular mechanisms: receptor phosphorylation, binding to a cytosolic regulatory protein, and receptor sequestration-internalization (Hausdorff et al., 1990). Serine-threonine phosphorylation at multiple sites on the βAR by type 2 G protein receptor kinases (GRK2) results in an early phase of βAR desensitization (Hausdorff et al., 1991, Hausdorff et al., 1990, Lefkowitz, 1993). With continued stimulation, this control is supplemented by binding to a soluble regulatory protein, β-arrestin (Lohse et al., 1990), and by sequestration at or near the plasma membrane, followed by internalization of the receptor into endosomes (vonZastrow and Kobilka, 1992), and finally, by degradation in the lysosomes..

The muscarinic cholinergic receptor is a 7 TMD receptor which is distributed diffusely throughout the cortex, but has a high density in deep structures of the brain, including in the pyramidal cell layer of the hippocampus (Buckley et al., 1988). The hippocampus is a crossroad for memory processing, and the muscarinic receptors are postulated to participate in inhibition of transmission during memory formation (Hasselmo and Bower, 1993). It is likely that this receptor is carefully regulated like other neurotransmitter receptors, including regulation by receptor desensitization. Based on ligand binding studies, regulation of the muscarinic receptor by sequestration-internalization has been established (Koenig and Edwardson, 1994, Liles et al., 1985), though the extent of this control is dependent on the cell type examined. Whether muscarinic receptor is also phosphorylated in response to agonist is less clear, and may be related to the subtype of receptor examined. Five subtypes of muscarinic receptors have been cloned to date (m1-m5) (Bonner et al., 1987). Of these subtypes, m2 and m4 are related by a common effector pathway (adenylyl cyclase inhibition) and m1, 3, and 5 are similar by virtue of their action on the the phospholipase C-phosphatidyl inositol (PLC-PI) pathway. The m3 receptor is rapidly and extensively phosphorylated upon agonist exposure in transfected cells (Tobin and Nahorski, 1993). The endogenous m1 receptor from porcine brain is phosphorylated *in vitro* by protein kinase C (PKC, Uchiyama et al., 1990), though the transfected m1 is not a PKC substrate in other systems (Richardson and Hosey, 1992). Finally, in N1E-115 neuroblastoma cells, PKC activation results in muscarinic receptor internalization and downregulation, which suggests a link between these two

mechanisms (Liles et al., 1985). To investigate the processes which are potentially associated with human m1 muscarinic receptor desensitization, we sought first to obtain physical evidence that the human m1 receptor (Hm1) is phosphorylated in response to agonist. To document receptor phosphorylation, we chose to isolate the phosphorylated m1 receptor by immunoprecipitating it from transfected cells. (The second part of this project, demonstration of agonist-induced receptor internalization, which might also be associated with m1 desensitiztion, will be described in the Chapter 3.) In this way we sought to determine if the same processes which appear to mediate desensitization of the βAR also functioned in the regulation of Hm1.

## EXPERIMENTAL PROCEDURE

### Materials

[$^3$H]-N-methyl scopolamine ([$^3$H]-NMS, specific activity 85 Ci/mmol) and [$^3$H]-quinuclidinyl benzoate ([$^3$H]-QNB, specific activity 47 Ci/mmol) was obtained from Amersham Corp. Digitonin was from Wako Industries (Richmond, VA) and deoxcholate from Sigma (St. Louis, MO). All other reagents were of analytical grade quality from common commercial sources. Restriction enzymes were from Boehringer Mannheim or Bethesda Research Laboratories.

Digitonin was prepared by diluting powdered pure reagent in water to make a 5% stock. The solution was heated to 95°C for ~20 minutes until the digitonin was in solution. The solution was all-

lowed to cool and stored at 4°C protected from light. Insoluble material if present was filtered prior to use. Detergent solution was stable for ten days according to the manufacturer's report.

Anti-epitope monoclonal antibodies (anti-EE mAb, (Grussenmeyer et al., 1985)) were used with the permission of Gernot Walter (University of California, San Diego) and purchased from Onyx Inc. (Richmond, CA). FITC-conjugated anti-mouse IgG antibodies were purchased from Cappell Technika (Durham, North Carolina).

**Epitope Tag and Stable Expression of Hm1**

The gene encoding Hm1 was obtained from a human placental genomic library as previously described (Maeda et al., 1990). A 5' primer for the human muscarinic cholinergic receptor type 1 (Hm1) was synthesized: TGAATTCACCATGGAATACATGCCAATGGAAAACACT TCAGCCCCACCTGCTGTC which contained the following components: an *EcoRI* restriction site, a three-nucleotide spacer, an initiating methionine, the sequence coding for the epitope EYMPME (underlined), followed by Hm1 sequence. The 3' primer (TTGGCGCCTGCTCGGTTC TCTGTCTCCCGGTA), contained a *BamH1* restriction site and allowed amplification of the epitope-tagged Hm1 (EE-Hm1) by polymerase chain reaction. The double-digested PCR product was ligated into pSG5 and the construct was transfected into DH5α by electroporation (BioRad GenePulser, Hercules, CA)). The sequence of the selected clone was verified, and the plasmid was co-transfected with a neomycin-resistance gene ($pRSV^{neo}$) into human embryonic kidney (HEK 293) cells by the calcium phosphate precipitation method with

dimethyl sulfoxide shock. Clonal cell lines expressing EE-Hm1 sites were selected in DMEM/H-16/F-12 with 10% FCS, 1% penicillin/streptomycin and 400 μg/ml G-418 in 5% $CO_2$/95% air, and maintained in this medium containing 200 μg/ml G-418. Clones with >4 x$10^5$ sites/cell as determined by [$^3$H]-NMS binding were selected for further experiments. Untagged wild-type Hm1 receptor was stably expressed in HEK 293 cells following the same transfection and selection protocol as for the epitope-tagged receptor.

To determine if the epitope tag affected the binding or function of the Hm1 receptor, HEK 293 cells stably expressing Hm1 lacking an amino-terminal epitope were compared to epitope-tagged cells. The procedure for stable expression is described in (Moro et al., 1994) and is similar to that described for epitope-tagged Hm1 expression. This cell line was maintained under the same selection conditions as EE-Hm1 cells.

**Ligand Binding and Phosphatidyl Inositol Turnover Studies**

Ligand binding studies were performed with EE-Hm1 cells as described in (Lameh et al., 1992). Phosphatidyl inositol turnover was measured as in (Berridge et al., 1982) and is described in Chapter 4.

**Receptor Purification and Immunoprecipitation**

Confluent flasks with 2 x $10^7$ HEK 293 cells stably expressing EE-Hm1 were washed briefly with PBS and incubated with lysis buffer (5 mM Tris, pH 7.4, 2 mM EDTA, 1 mM EGTA, 1 mM PMSF, 1 μg/ml leupeptin, 1 μg/ml aprotinin) for 10 minutes on ice. The pro-

tocol for isolating membranes is as described in Chapter 1 for the epitope-tagged μ-opioid receptor (Chapter 1)except that cells were disrupted by aspirating and expelling through a 25 g needle rather than in a Dounce homogenizer.

The EE-Hm1 was solubilized in 1% digitonin, 0.2% deoxycholate as described (Wall et al., 1991). Briefly, membrane pellets were first labelled with 1 nM [$^3$H]-QNB for 2 hour at 4°C, resuspended in solubilization buffer (10 mM Tris (pH 7.4), 100mM NaCl, 2 mM EDTA, 2 mM EGTA, 1% digitonin, 0.2% deoxycholate, 1 mM PMSF, 1 μg/ml leupeptin, 1 μg/ml aprotinin) and incubated for 30 minutes at 4°C with gentle vortexing. The reaction mixture was centrifuged at 105,000 x g for 40 minutes at 4°C and the supernatant was applied to a sephadex G-50 (superfine) gel filtration column pre-equilibrated with 10 mM Tris, 160 mM NaCl, 1 mM EDTA, 0.1% digitonin, 0.02% deoxycholate. Fractions (2 minute intervals) were collected and the $^3$H content of 25 μl aliquots was determined in 5 ml Scintiverse II (Fisher Biotech, Pittsburgh, PA).

For immunoprecipitation of EE-Hm1, membrane pellets were first resuspended in Tris-NaCl buffer including the protease inhibitors described above, and labelled with 1 nM [$^3$H]-QNB for 2 hours at 4°C. Membranes were centrifuged at 30,000 x g for 20 minutes, and the pellet was resuspended in solubilization buffer containing 1% digitonin and 0.2% deoxycholate. After gentle mixing for 30 minutes the solution was centrifuged at 105,000 x g for 40 minutes. The supernatant, containing detergent-solubilized membrane, was incubated with a 1:50 dilution of anti-EE mAb and 30 μl of a 50% slurry of washed protein G sepharose 4 fast flow for 12 hr.

Beads were washed in cold Tris-NaCl buffer without detergent and were harvested on GF/C filters pretreated with 0.3% polyethyleneimine. Filters were washed three times with ice-cold PBS and counted. Protein determination was by the method of Bradford (Bradford, 1976).

Phosphorylation of EE-Hm1 was performed as described in Chapter 1 for EE-μR by labellling digitonin-permebilized EE-Hm1 cells with 1 μCi/μl [$\gamma$-$^{32}$P]-ATP (7000 Ci/mmol, Dupont/NEN, Boston, MA) for 15 minutes at 25°C in the presence or absence of 1 mM carbachol. Cells were then washed three times in cold buffer consisting of 10 mM potassium phosphate (pH 7.4), 5 mM EDTA, 10 mM NaF, 10 mM sodium pyrophosphate and protease inhibitors (1 mM PMSF, 1 μg/ml leupeptin, 1 μg/ml aprotinin) by incubating for 10 minutes on ice in cold lysis buffer, disruption by passage through a 25 g needle, followed by differential centrifugation to give crude membrane. Membranes were solubilized and immunoprecipitation was performed as described above. After the phosphorylated receptor was immunoprecipitated, beads were washed three times with solubilization buffer and resuspended in 1 ml of cold PBS. The reaction was colllected on GF/C filters which were washed with cold PBS. The $^{32}$P content of the GF/C glass filters and of the filter wash was determined in 5 ml of scintillation fluid.

## RESULTS

### Expression and Function of Epitope-Tagged Hm1

Sixteen clones co-transfected with EE-Hm1 and pRSV$^{neo}$ were selected for screening by measuring binding to [$^3$H]-NMS. One transfected HEK 293 cell clone expressing the epitope-tagged Hm1 (EE-Hm1) at ~4 x $10^5$ sites/cell was characterized by saturation and displacement binding, and inositol phosphate turnover. There was no significant difference in binding maximum or inositol phosphate turnover between tagged and untagged receptor in stably-transfected cells at similar levels of expression. Maximum binding by EE-Hm1 was 3.9 pmoles/mg protein and for Hm1 the binding maximum was 3.4 pmoles/mg protein. Maximal inositol phosphate release was attained with 10 μM carbachol (EE-Hm1: 15.6 ± 1 fold control; Hm1: 13.4 ± 4 fold control) with no additional stimulation at 1 mM carbachol. A small, but significant, decrease in affinity for carbachol was observed for EE-Hm1 compared to Hm1 in [$^3$H]-NMS displacement studies. Binding and PI turnover data are summarized in Chapter 3, Table I.

In antibody competition studies, [$^3$H]-NMS binding was unchanged from control binding even at antibody dilutions as low as 1:10. Antibody-receptor interaction did not result in functional coupling of tagged receptor, since monoclonal antibody anti-EE at low dilution (1:10) did not stimulate release of inositol phosphate (data not shown).

**Solubilization of Epitope-tagged and Untagged Hm1**

When cells were labelled with [$^3$H]-QNB and membranes were harvested and solubilized in 1% digitonin and 0.2% deoxycholate, both ligand bound Hm1 and ligand bound EE-Hm1 could be separated from free [$^3$H]-QNB by gel filtration chromatography (Figure 2.1). Approximately 791 fmoles of [$^3$H]-QNB binding activity and 756 fmole of [$^3$H]-QNB binding activity were recovered from 2 x $10^7$ Hm1 and EE-Hm1 cells, respectively. Calculations based on total ligand binding indicates that digitonin/deoxycholate solubilized 6.1% of Hm1 and 5.8% of EE-Hm1.

**Immunoprecipitation and Phosphorylation of Epitope-Tagged Hm1**

Ligand bound EE-Hm1 which was solubilized in detergent was immunoprecipitated by anti-EE mAb and protein G Sepharose beads. Data from experiments comparing the immunoprecipitation of EE-Hm1, Hm1, and untransfected HEK 293 cells are shown in Figure 2.2. Immunoprecipitation of EE-Hm1 yielded 125.6 fmoles of receptor from 2 x $10^7$ cells, which is approximately 17% of solubilized EE-Hm1. Non-specific binding of the highly lipophilic ligand $^3$H-QNB accounted for 11.5 fmoles of binding in untagged Hm1 expressing cells and for 26.6 fmoles of binding in HEK 293 cells. Overall, solubilization and immunoprecipitation resulted in the purification of ~1.2% of EE-Hm1, as defined by [$^3$H]-QNB binding activity.

Incorporation of $^{32}$P by EE-Hm1 was 3.1 ± 0.3 times the background incorporation of $^{32}$P by untransfected HEK 293 cells (n = 3). There was no difference in phosphorylation between immunoprecipi-

tates from carbachol-treated and untreated cells. Supernatants from the immunoprecipitation of labeled EE-Hm1 and from untransfected cells contained similar $^{32}P$ levels.

## DISCUSSION

The purpose of these experiments was to determine if Hm1 is phosphorylated in response to agonist, and to relate this biochemical modification to the internalization of the Hm1. Alanine mutation of a serine and threonine-rich domain (SLTSS→ALAAA) in the i3-loop of Hm1 (287-291) (Moro et al., 1994) had resulted in a complete failure to internalize in response to carbachol (98% of unstimulated cell binding). An analogous mutation in Hm3 had resulted in a similar defect in agonist-induced internalization. The hypothesis that this region was the substrate domain for a regulatory serine-threonine kinase resulted in the experiments presented here, designed to identify phosphorylated Hm1 by immunoprecipitation.

Purification of the m1 receptor is reported by chromatography on a ligand affinity column (Haga and Haga, 1985) and by immunoprecipitation (Mayanil et al., 1989, Wall et al., 1991). Since the large hydrophobic i3 loop was the focus of the mutational analysis of Hm1 internalization, another antigenic domain was required. Antibodies raised against the a C-terminal peptide (Wall et al., 1991) had not been useful in separating sufficient quantities of purified receptor to identify on SDS-PAGE. We duplicated this approach with similar results. Consequently, we added an amino-terminal epitope tag to the

Hm1 and stably expressed the tagged receptor (EE-Hm1) in HEK 293 cells. The corresponding monoclonal antibody was used to immunoprecipitate the receptor and to identify Hm1 by immunofluorescence microscopy (Chapter 3).

EE-Hm1 was well expressed in HEK 293 cells based in [$^3$H]-NMS binding, and the epitope-tagged receptor was fully functional by assay of inositol phosphate hydrolysis. The small decrease in EE-Hm1 affinity in [$^3$H]-NMS displacement studies suggests that the addition of the extracellular epitope may exert a small effect on the ligand binding properties of the receptor at the cell surface. The anti-EE monoclonal antibody neither competed with a cholinergic antagonist for ligand binding sites nor interfered with normal signal transduction. Detergent solubilization of both the endogenous and the transfected receptor was with digitonin (Richardson et al., 1991, Wall et al., 1991) and we found digitonin plus deoxycholate solubilized the receptor in a native, ligand bound conformation. However, the percentage of total receptors that were solubilized with digitonin was low, and screening of other detergents was hampered by the lack of a repeatable, specific detection method for solubilized Hm1. Use of an alkylating antagonist to the m1 receptor such as [$^3$H]-propylbenzilylcholine mustard, which labels the third transmembrane domain of the muscarinic receptor (Curtis et al., 1989, Uchiyama et al., 1990), could provide a means of identifying Hm1 under more stringent solubilzation conditions. This compound was not available for these studies. Poor solubilization of the Hm1 might be partially circumvented by improved expression of the receptor. An increase in the number of solubilized receptors may facilitate

detection by immunoblotting and improve the yield of immunoprecipitation. Higher levels of expression have been achieved for the EE-μ opioid receptor (EE-μR) in HEK 293 cells (Chapter 1), and this may be attributed in part to the vector (pRC for EE-μR, pSG5 for EE-Hm1) used for the EE-μR construct.

The EE-Hm1 was specifically immunoprecipitated by anti-EE mAb. This result and those presented for the epitope-tagged opioid receptor in Chapter 1 indicate the utility of epitope-tagging proteins for immunoprecipitation. The affinity of the antibody appears to be low however, since relatively low dilutions (1:50) were needed for immunoprecipitation. Moreover, the combination of low efficiency solubilization of EE-Hm1 and a low affinity antibody resulted in a low recovery of EE-Hm1 by immunoprecipitation (~1.2% of total [$^3$H]-NMS binding).

Agonist-induced phosphorylation of the m1 receptor has not been documented. Phosphorylation by protein kinase C in vitro was reported (Uchiyama et al., 1990) but m1, unlike other subtypes of muscarinic receptors was not phosphorylated by protein kinase C in transfected Sf9 insect cells (Richardson and Hosey, 1992). A $^{32}$P signal was detectable in EE-Hm1 immunoprecipitates, but we could not demonstrate any change in receptor phosphorylation induced by agonist stimulation. The change in receptor phosphorylation for G protein coupled receptors is variable following a 15 minute agonist exposure: the m3 muscarinic receptor $^{32}$P incorporation increased by 10 times (Tobin and Nahorski, 1993), but the 5-HT$_{1A}$ receptor incorporation increased by only 3 times (Raymond, 1991). Phosphorylation of the μ-opioid receptor increased only 1.7 times

over control (see Chapter 1). Thus its is possible that Hm1 phosphorylation may be enhanced by agonist stimulation, but the enhancement may be very small, and would likely be undetectable by the method described here, considering the efficiency of the purification procedure for EE-Hm1.

In conclusion, we have modified the Hm1 receptor by adding an epitope at the amino terminus, and have specifically immunoprecipitated it in from transfected cells. Immunoprecipitated receptors are phosphorylated in the resting state, though agonist-enhanced phosphorylation was not demonstrated. Delineation of the Hm1 phosphorylation sites and of the relationship of this modification, if any exists, to receptor internalization, will require a higher level of Hm1 expression and a more efficient solubilization and immunoprecipitation strategy.

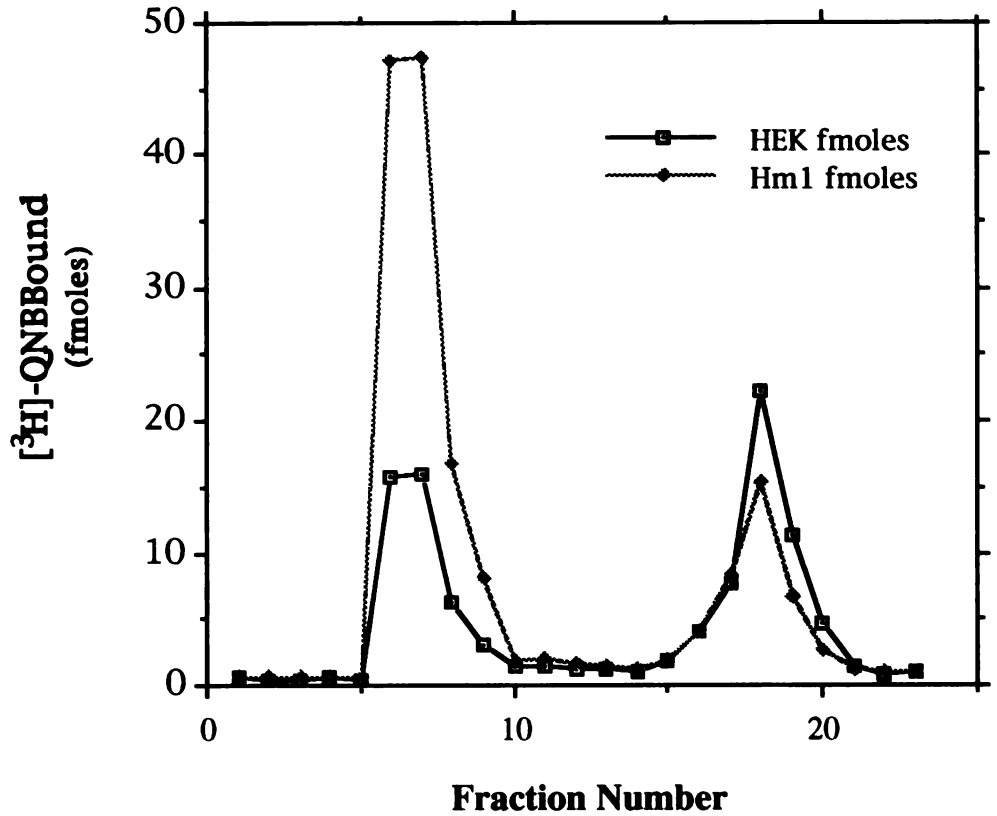


Figure 2.1. Solubilization of Hm1 from stably transfected HEK 293 cells. Cells were lysed and membranes prepared as in "Experimental Procedures" and solubilized receptor was separated from free [$^3$H]-QNB by gel filtration chromatography. Fractions were collected at two minute intervals. The plot for EE-Hm1 was similar to the plot for Hm1.

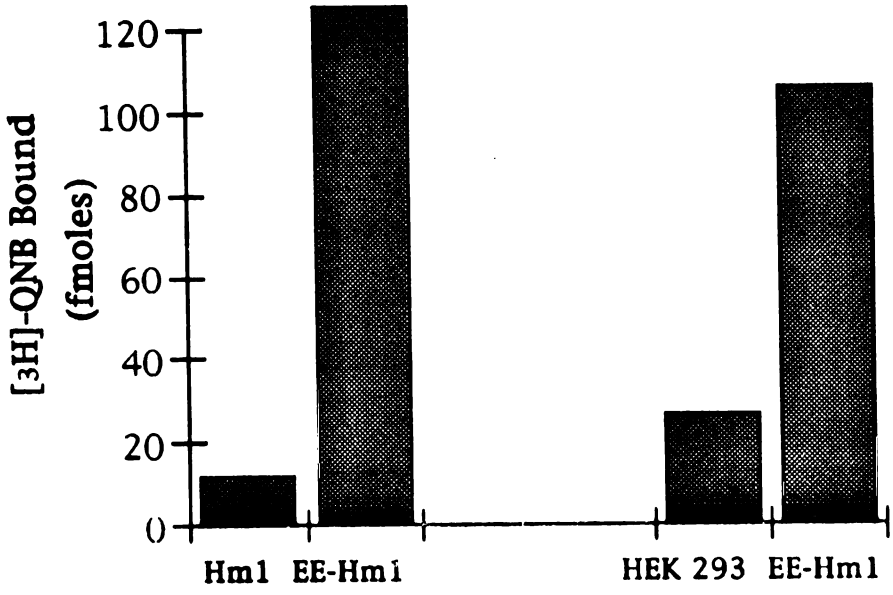


Figure 2.2 Immunoprecipitation EE-Hm1 with bound [$^3$H]-QNB. In two separate experiments, cells stably transfected with EE-Hm1 (EE-Hm1) were compared to cells transfected with untagged Hm1 (Hm1) or untransfected cells (HEK 293). Cells were labeled with [$^3$H]-QNB as described, and detergent-solubilized membranes was incubated for 12 hours at 4$^o$C with anti-EE mAb and protein G Sepharose beads. Immunoprecipitates were collected on glass filters and the amount of bound [$^3$H]-QNB was determined.

# CHAPTER 3

# MUTATIONS IN THE CYTOPLASMIC LOOPS OF THE HUMAN M1 MUSCARINIC RECEPTOR INHIBIT INTERNALIZATION:

## CONFOCAL MICROSCOPY IN PERMEABILIZED AND SYNCHRONIZED CELLS


## SUMMARY

We have previously described (Lameh et al., 1992, Moro et al., 1994) two cytoplasmic loop mutants of the human m1 muscarinic cholinergic receptor (Hm1): Hm1-(V127A/L131A), which is functionally uncoupled and completely defective in internalization; and Hm1-(d232-358), which is highly deficient in internalization, but is G protein-coupled. Using an amino-terminal epitope tag (EYMPME) and immunofluorescence confocal microscopy, we have examined agonist-induced internalization of tagged wild type (EE-Hm1) and tagged cytoplasmic loop mutants of Hm1. When EE-Hm1 was treated with 1 mM carbachol, cytoplasmic vesicles containing EE-Hm1 appeared within 5 minutes and accumulated in the cytoplasm over the next 40-minutes. Mutant V127AL131A showed no evidence of agonist-induced receptor internalization. In contast, carbachol induced

internalization of the d232-358 mutant, although this process appeared to be slower than observed for wild-type receptor. In synchronized endocytosis resulting from a temperature shift, the early phase of internalization was slower in d232-358 compared to wild-type. These results present a highly sensitive and specific method for following receptor internalization, and give morphological support for a relationship in Hm1 between G protein coupling ability and agonist-induced receptor internalization.

## INTRODUCTION

The m1 subtype of the human muscarinic cholinergic receptor (Hm1) is a prominent receptor subtype in the central nervous system, and is a member of the G protein-coupled, seven transmembrane domain (7 TMD) receptor family. Rapid regulation of neurotransmitter receptors is critical to the modulation of cell signaling, and the regulation of 7 TMD receptors in the central nervous system has been intensively studied. Desensitization of the $\beta_2$-adrenergic receptor ($\beta_2$AR) is one of the best characterized regulatory processes to date (Hausdorff et al., 1990). Both biochemical modifications, such as receptor phosphorylation (Hausdorff et al., 1989), and cell biological processes, such as receptor sequestration and recycling (vonZastrow and Kobilka, 1994, vonZastrow and Kobilka, 1992), appear to contribute to the desensitization of the of the $\beta_2$AR. Although the $\beta_2$AR has been carefully examined, much less is known about the desensitization of the muscarinic cholinergic receptors.

Phosphorylation of the m1 receptor by protein kinase C has been demonstrated *in vitro* (Haga et al., 1990, Uchiyama et al., 1990), but phosphorylation of transfected Hm1 is uncertain (Richardson and Hosey, 1992). Data on the internalization of the endogenous muscarinic receptor from ligand binding studies indicate that the receptor is internalized (Lameh et al., 1992, Maeda et al., 1990, Maloteaux and Hermans, 1994, Slowiejko et al., 1994). The available morphological data, however, suggest that Hm1 appears in invagination of the plasma membrane or in a compartment just beneath the plasma membrane following agonist exposure (Raposo et al., 1987).

In the present study, we have stably expressed an epitope-tagged Hm1 receptor in HEK 293 cells. The epitope-tagged receptor (EE-Hm1) is similar to the untagged receptor in ligand binding and in coupling to downstream effectors. When visualized by immunofluorescence confocal laser microscopy, the receptor internalized rapidly following agonist exposure. A large deletion of the third cytoplasmic domain of the receptor, which significantly decreased agonist-induced internalization, as evidenced by ligand binding studies (Lameh et al., 1992), did not completely block internalization, but rather slowed this process. In contrast, double point mutation in the second cytoplasmic loop, which resulted in an internalization- and coupling-defective receptor (Moro et al., 1994), completely blocked agonist-induced receptor internalization.

## EXPERIMENTAL PROCEDURES

### Materials

[$^3$H]-N-methyl scopolamine ([$^3$H]-NMS, specific activity 85 Ci/mmol) and [$^3$H]-quinuclidinyl benzoate ([$^3$H]-QNB, specific activity 47 Ci/mmol) was obtained from Amersham Corp. Fish gelatin, poly-L-lysine, carbachol were purchased from Sigma Chemical Co (St. Louis, MO), and Fluoromount G from Fisher Scientific (Pittsburgh, PA). All other reagents were of analytical grade quality from common commercial sources. Restriction enzymes were from Boehringer Mannheim or Bethesda Research Laboratories.

Monoclonal antibodies to the epitope EYMPME (anti-EE mAb, (Grussenmeyer et al., 1985) were used with the permission of Gernot Walter (University of California, San Diego) and purchased from Onyx Inc. (Richmond, CA). FITC-conjugated anti-mouse IgG antibodies were purchased from Cappell Technika (Durham, North Carolina).

### Epitope Tag and Stable Expression of Hm1

The procedure for the addition of an amino-terminal epitope tag for the human muscarinic receptor (Hm1) is described in the Chapter 2. Clonal cell lines expressing the epitope-tagged receptor (EE-Hm1) were selected and maintained as described.

### Epitope-tagged mutants of Hm1

Deletion mutation of the third intracellular loop of the Hm1 was introduced as described previously (Lameh et al., 1992). Briefly, Hm1 in the vector Gem3 was cut at the unique *StuI* restriction site in

the third intracellular loop and digested with Bal-31 for varying lengths of time at 4°C. Following self-ligation of blunt-end products, mutants were sequenced, in-frame mutants were digested with *Bam HI* and *EcoRI*, and the product was subcloned into the vector pSG5. One mutant, d232-358, which was a deletion of a large portion of the third cytoplasmic loop, has been characterized previously (Arden et al., 1992, Lameh et al., 1992, Maeda et al., 1990) and was examined in this study. Point mutations of the i2-loop of Hm1 (V127A/L131A) were introduced by the unique site elimination method as described in Moro et al., 1993 (Moro et al., 1993). Epitope-tagged deletion mutants were constructed by double digesting to isolate the mutation, and ligating the fragment into the a similarly digested, epitope-tagged wild-type Hm1 sequence. The presence of the mutations in the constructs was confirmed by sequencing. We thereby constructed the tagged mutants EE-(d232-358) and EE-(V127/L131A).

**Receptor Binding, Internalization and Inositol Phosphate Assay**

Binding to the hydrophilic ligand [$^3$H]-N-methyl scopolamine was used to quantitate EE-Hm1 surface expression and displacement binding curves with carbachol or NMS were performed as described by Lameh et al. (Lameh et al., 1992). Carbachol displacement data were fit to the logistic function, B = Bmax - [Bmin * L]/ [IC50 + L] + NSB, where B is the tracer bound, L = carbachol concentration and NSB is the nonspecific binding. Receptor internalization was quantitated by plating cells on 12-well cell culture dishes and allowing

them to attach overnight. Cells were then incubated with 1 mM carbachol or with buffer for various times at 37°C, washed three times in ice cold PBS and incubated with 1.5 nM [$^3$H]-NMS at 12°C for 90 min. At the end of labeling, cells were placed on ice, harvested in PBS, and filtered on glass-fiber filters, followed by three rinses with ice-cold PBS. Agonist-induced release of inositol phosphate was measured by the method of Berridge et al. (Berridge et al., 1982). Briefly, cells at a density of 1.5 x $10^6$ cells/ml medium were labeled in triplicate wells for 24 h with [$^3$H]-*myo*-inositol. After incubating with LiCl, cells were exposed to differing concentrations of agonist, and the reaction was terminated by removing the medium and fixing the cells with methanol. Cells were harvested, extracted in chloroform and water, and the water soluble fraction was passed through an anion-exchange resin (AG 1-X8, formate form, BioRad, Hercules, CA), washed, eluted with ammonium formate/formate buffer and counted. Agonist-induced stimulation of inositol phosphate release was expressed as multiples of baseline inositol phosphate release in untreated cells.

Statistical comparison of values for epitope-tagged and untagged receptor was performed by two-tailed t-test using a pooled-variance estimate and a level of significance of $p < 0.05$ (Glantz, 1981; Zar, 1974).

**Confocal Laser Microscopy of EE-Hm1 Internalization**

For time-course studies, EE-Hm1/HEK 293 cells were grown overnight at low density in complete medium on chamber slides

(Nunc Inc., Napperville, IL) pre-treated with poly-L-lysine. Cells were exposed to carbachol or buffer for specified times in complete medium at 37°C. Cells were washed once at room temperature with PBS, fixed for 10 minutes in PBS containing 3.7% paraformaldehyde, and permeabilized in PBS containing 0.25% cold water fish gelatin, 0.04% saponin and 0.05% $NaN_3$ (IMF/saponin buffer). After incubation for 1 hour with 1:1000 anti-EE mAb in IMF/saponin buffer, cells were washed four times in PBS and incubated with 1:4000 FITC-conjugated anti-mouse antibody in IMF/saponin buffer for 30 minutes, washed three times with PBS and once with water, mounted with Fluoromount G containing trace *p*-phenylene diamine under coverslips, and stored at 4°C. The specificity of immunofluorescence staining was confirmed by the absence of an epitope signal in untransfected HEK 293 cells and in cells stained with secondary antibody alone.

For synchronized internalization studies, cells grown overnight on slide chambers were first cooled for 10 minutes at 0-4°C. Complete medium was then replaced by serum-free medium containing 1:1000 anti-EE mAb and 1 mM carbachol in IMF/saponin buffer. Cells were incubated for 50 minutes at 4°C and were then warmed to 37°C in a water bath for the specified times, re-cooled on ice and the medium was immediately replaced with cold medium. Cells were washed with cold PBS and fixed for 5 minutes on ice then for 10 minutes at room temperature. Indirect immunofluorescence was performed as described, using FITC-conjugated secondary antibody.

Cells were visualized using a krypton-argon laser coupled with a BioRad MRC-600 confocal head attached to a Optiphot II Nikon microscope with a Plan Apo 60X 1.4 NA objective lens. Samples were scanned for FITC emission using a blue high sensitivity filter block. Collection parameters were 3 s/scan, 7 frames/image, Kalman filter, motor step size 0.5 μm, diaphragm one-third open. Optical sections along the z-axis of isolated cells were stored on 940 MB optical disc (Panasonic Inc). Images from the central plane of the cell were compared to assess internalization/sequestration.

## RESULTS

### Expression and Function of Epitope-Tagged Hm1

Sixteen clones co-transfected with EE-Hm1 and pRSV$^{neo}$ were selected for screening by measuring binding to the hydrophilic antagonist [$^3$H]-N-methyl scopolamine ([$^3$H]-NMS). One transfected HEK 293 cell clone expressing the epitope-tagged Hm1 (EE-Hm1) at ~4 x $10^5$ sites/cell was characterized by saturation and displacement binding, and inositol phosphate turnover. Data for cells stably expressing epitope-tagged or untagged Hm1 are in Table I. There was no significant difference in binding maximum between tagged and untagged receptors in stably-transfected cells at similar levels of expression. In [$^3$H]-NMS displacement studies a small, but significantly lower, affinity for carbachol was observed for EE-Hm1 as compared to untagged Hm1 (IC50 3.3 ± 0.7 and 1.6 ± 0.4, respectively). Cells stably transfected with tagged or untagged Hm1 receptor had similar

degrees of inositol phosphate stimulation following carbachol stimulation. Maximal inositol phosphate release was attained with 10 μM carbachol (EE-Hm1: 15.6 ± 1 fold control; Hm1: 13.4 ± 4 fold control) with no additional stimulation at 1mM carbachol.

Exonuclease digestion of the third cytoplasmic loop (i3 loop) of Hm1 at the unique *StuI* site resulted in deletions of different lengths as previously described (Arden et al., 1992, Lameh et al., 1992, Maeda et al., 1990). The largest of these deletions (d232-358) was shown to be similar to wild-type Hm1 in ligand binding and to be fully active in carbachol-stimulated inositol phosphate release (Arden et al., 1992). The addition of the epitope to the i3-loop deletion mutant of Hm1 (EE-d232-358) was expressed at a level similar to that of the wild type receptor (~4 x $10^5$ sites/cell) and was fully functional in inositol phosphate release.

The i2-loop double point mutant (EE-V127A/L131A) stably expressed in HEK 293 cells expressed ~200,000 sites /cell by [$^3$H]-NMS binding. The V127A/L131A mutant was previously reported to be uncoupled from G protein effectors with only 8% of maximal phosphoinositide release of wild-type Hm1 (Moro et al., 1994).

**Hm1 internalization: ligand binding and laser confocal microscopy**

EE-Hm1 and EE-(d232-358) had 67% and 85% of pretreatment [$^3$H]-NMS binding respectively, following 15 minute carbachol exposure. Binding of [$^3$H]-NMS to EE-(V127A/L131A) was unaffected by exposure to carbachol as predicted from the defective internalization

reported for the untagged double point mutant (100 ± 2% control) (Moro et al., 1994).

The anti-epitope monoclonal antibody (anti-EE mAb) labeled EE-Hm1 surface receptors on both permeabilized and unpermeabilized cells. In unstimulated, permeabilized cells, intense staining was visible at the plasma membrane. In these cells, scattered areas of punctate staining were also observed on optical sections of the cytoplasm (Figure 3.1a). Both the intensity and distribution of this punctate cytoplasmic staining changed with increasing time of exposure to agonist. After 5 minutes of exposure to carbachol more scattered intracellular vesicles were visible in the periphery (Figure 3.1b). The number of cytoplasmic vesicles increased to give a more intense and concentrated intracellular signal as agonist exposure time increased (Figures 3.1c, d). Intracellular signal intensity reached peak levels following approximately 30 minutes of agonist exposure (Figure 3.1e), with little enhancement in cytoplasmic signal intensity following longer incubation with agonist (Figure 3.1f).

Prior to agonist exposure the i3-loop deletion mutant (EE-d232-358) was found primarily at the cell surface with scattered punctate signals visible in the cytoplasm (Figure 3.2a). This pattern of staining was not changed at 5, 10 and 15 minutes of agonist exposure (Figure 3.2b, c, d). After 30 minutes of carbachol treatment, the EE-d232-358 was found in cytoplasmic vesicles (Figure 3.2e). The deletion mutant receptor was found in numerous intensely-staining cytoplasmic vesicles after 30 minutes and in intensely-staining vesicles after 40 minutes of agonist exposure (Figure 3.2f).

The EE-V127A/L131A mutant remained at the cell surface throughout the 30 minute agonist treatment (Figure 3.3a, b). This observation confirms ligand binding studies which showed that the V127A/L131A mutant fails to internalize following agonist exposure.

**Synchronized internalization of EE-Hm1**

A scattered punctated staining was visible in permeabilized EE-Hm1 transfected cells prior to agonist stimulation. This punctate pattern in the resting state could represent Hm1 receptor involved in several different cellular processes. To distinguish internalization from the other processes, we isolated a population of EE-Hm1 receptors at the cell surface by incubating the cells in the presence of anti-EE mAb at 4°C for 20 minutes with and without agonist. To observe a single population of Hm1 during internalization, we washed the cells at 4°C to remove unbound antibody and agonist, and warmed them for different periods of time at 37°C prior to re-cooling. To observe a continuum of Hm1 internalization, cells were exposed to antibody and carbachol throughout the warming periods prior to re-cooling. In this way the intracellular movement of a synchronized population of surface EE-Hm1 could be visualized in the absence of interfering signals from receptors which were either in transit to the cell membrane or were in a resting intracellular compartment.

Following incubation with 1 mM carbachol and 1:1000 anti-EE mAb at 4°C, a circumferential staining pattern without a cytoplasmic signal was visualized by confocal microscopy (Figure 3.4a). After 2 minutes of warming the uniform, circumferential pattern became ir-

regular, and at 4 minutes a small pattern of punctate staining appeared just below the plasma membrane (Figure 3.4b). With longer periods of warming, the vesicular cytoplasmic staining increased in intensity and, after 20 minutes, concentrated into bright cytoplasmic densities (Figure 3.4c). The time course of internalization and the appearance of this population of vesicles were the same, regardless of whether the cells were continuously exposed to antibody and agonist during warming, or whether they were washed extensively prior to warming.

After cooling to 4°C and incubating with 1 mM carbachol anti-EE mAb, the i3-loop deletion mutant showed a circumferential pattern of plasma membrane staining similar to that observed for wild-type receptor (Figure 3.4d). However the early phase of receptor internalization was delayed in the deletion mutant since no punctate intracellular staining was apparent after 4 minutes of warming (Figure 3.4e). By 15 minutes of warming an intense pattern of cytoplasmic vesicle staining was apparent (Figure 3.4f) which was similar to the wild type receptor after shorter periods of warming, indicating that the large deletion in the i3 loop resulted in slowed, but not defective, internalization.

## DISCUSSION

### Agonist-induced Hm1 internalization

In previous work (Lameh et al., 1992) with HEK 293 cells stably-transfected with Hm1, treatment for 15 minutes with 1 mM car-

bachol resulted in a decrease of [$^3$H]-NMS surface binding to 55% of pretreatment binding after 2 hours, with no further loss of tracer binding after longer chase times. Lipophilic ligand binding ([$^3$H]-QNB) was unaffected by carbachol treatment, implying that the loss of [$^3$H]-NMS binding reflected internalization-sequestration of Hm1 rather than receptor downregulation. In the present study we have verified that carbachol-stimulated receptor internalization-sequestration is similar to that described previously for untagged receptor. In addition we have shown that epitope-tagged receptors couple to downstream effector pathways like untagged receptors.

Agonist-induced receptor internalization has been demonstrated morphologically for seven transmembrane spanning receptors. Raposo et al. (Raposo et al., 1989) visualized the βAR in cytoplasmic vesicles on electron micrographs and by immunofluorescence microscopy in permeabilized cells following exposure to isoproterenol. The kinetics of internalization, however, were not examined. Von Zastrow et al (vonZastrow and Kobilka, 1992), using confocal microscopy, found evidence of $\beta_2$AR internalization in response to agonist within 2 minutes of treatment. The receptor was rapidly internalized with no further enhancement of cytoplasmic vesicle staining apparent after 5 minutes of agonist exposure. These findings were in agreement with ligand binding studies of $\beta_2$AR internalization. In ligand binding studies of the endogenous muscarinic receptor (Maloteaux and Hermans, 1994, Slowiejko et al., 1994), loss of surface binding capacity was slower than for the adrenergic receptor, with maximal internalization occurring between 10 and 60 minutes after agonist exposure. Internalization of the muscarinic receptor in

transfected cells occurred within 10 minutes of agonist exposure in one report (Lameh et al., 1992). Morphological correlates to these muscarinic receptor binding studies are limited. Electron micrographs showed vesicles containing the muscarinic receptor in invaginations of the plasma membrane after 15 minutes of agonist exposure, with occasional cytoplasmic vesicles appearing after one hour of treatment (Raposo et al., 1987).

The micrographs presented here demonstrate that internalization of the muscarinic receptor is rapid following exposure to the agonist carbachol. The muscarinic receptor appears in cytoplasmic vesicles within 5 minutes of agonist exposure in permeabilized, unsynchronized cells, and continues to accumulate in these vesicles throughout the 40 minute agonist exposure period. Moreover, vesicles containing the receptor are widely distributed throughout the cytoplasm within approximately 5 minutes, rather than being confined to a compartment just beneath the plasma membrane. We found the rapid appearance of the muscarinic receptor following agonist exposure is a more specific description of early receptor internalization than ligand binding studies, which are technically difficult and give high variability at early time points (see Koenig and Edwardson, 1994, Figure 6 and Slowiejko et al., 1994, Figure 2).

The i2-loop mutant Hm1-(V127A/L131A) is internalization and coupling defective by binding and functional assays. Our data verify that this mutation completely blocks receptor internalization in response to agonist. Thus we have identified a critical site in the cytoplasmic loops which mediates Hm1 trafficking.

Binding assays for EE-(d232-358) mutant indicated that it was also internalization defective (Lameh et al., 1992), since it retained >98% of pretreatment [$^3$H]-NMS binding after 5 hr carbachol treatment. The i3-loop deletion did not result in uncoupling of the receptor since Hm1-(d232-358) retains wild-type G protein coupling (see Chapter 4). Confocal immunofluorescence micrographs clearly demonstrate that EE-(d232-358) does internalize, but that internalization occurs more slowly when compared to wild type receptor. These results support the proposal that internalization and Hm1 coupling are closely related processes. Thus, a mutation which results in uncoupling also disables internalization in EE-(V127A/L131A), while a mutation which does not prevent coupling also preserves internalization in EE-(d232-358). One could postulate that if EE-Hm1 recycles like the $\beta_2$AR (vonZastrow and Kobilka, 1994) and if d232-358 only delays internalization, then any internalized receptor would return to the cell surface at a normal rate, and it might appear as if little or no internalization had occurred.

The presence of cytoplasmic vesicles containing receptor in unstimulated cells could represent Hm1 during a number of intracellular processes, including transit to the surface following synthesis, spontaneous internalization, receptor recycling, residence in a cytoplasmic reserve compartment, or during lysosomal degradation. Trafficking of the muscarinic receptor in NG-108-15 cells has been modeled recently, based on ligand-binding studies (Koenig and Edwardson, 1994). The calculated half-time for agonist-induced internalization was 6.3 minutes, which agrees with the appearance of cytoplasmic vesicles we observed. In this model, the basal rate of

internalization is slow (half-time 26 minutes). However, since basal internalization rate is exponential and therefore, proportional to surface receptor number (Harden et al., 1985), a faster rate would be expected for the highly-expressed EE-Hm1, which might account for the presence of receptor in cytoplasmic vesicles which we observed in unstimulated cells. Inferences about the trafficking of EE-Hm1 based on the kinetic analysis of another similar, but endogenous, muscarinic subtype (m3) must be made cautiously.

**Synchronized Internalization of EE-Hm1**

Since the focus of this study was Hm1 internalization, we wished to follow the internalization of an isolated population of surface EE-Hm1 without interfering signals from other cytoplasmic EE-Hm1. We therefore antibody-loaded cells at 4°C and synchronized internalization by a temperature shift to 37°C. Sequential micrographs clearly document the time course of receptor transport into intracellular vesicles. EE-Hm1 internalization is rapid, with labeled receptors appearing throughout the cytoplasm within 4 minutes. The vesicles appear subjectively to be more consolidated after 10 minutes of warming, and this could reflect receptor sorting in the endosome. After 20 minutes of warming, the pattern of staining appears to be visible again at the cell periphery (Figure 3.4c), suggesting that EE-Hm1 may be recycling to the cell surface.

Recycling of the receptor to the cell surface after approximately 20 minutes of warming is in agreement with the plateau of the curve for m3 muscarinic receptor internalization in SH-SY-5Y cells, which occurred after approximately 20 minutes after a temperature shift to

37°C in the presence of agonist (Slowiejko et al., 1994). Recycling of the $\beta_2$AR has also been demonstrated by immunofluorescence microscopy using a protocol similar to that presented here (vonZastrow and Kobilka, 1994). Maximum internalization of the $\beta_2$-AR was observed after warming cells for approximately 10 minutes, with transit through the recycling pathway taking approximately 20 minutes.

The same pattern of internalization was seen regardless of whether the cells were washed at 4°C or not. While residual agonist, despite extensive washing, cannot be definitively ruled out, these results are consistent with the "committed step" model of $\beta_2$-AR internalization (vonZastrow and Kobilka, 1994). In this model agonist induces an early redistribution of the receptor into a membrane compartment from which the endocytic machinery, independent of agonist, transports it into endosomes. In the case of Hm1, incubation with agonist, even at 4°C, may be sufficient to induce the necessary conformational changes to commit it to this pathway.

We believe that the pattern of antibody staining which we observed during synchronized internalization accurately reflects the intracellular movement of the muscarinic receptor. It is unlikely that surface-bound antibody dissociates from the EE-Hm1 as endosomal pH decreases following internalization. Data from morphologic studies of the hCG/LH receptor (Ghinea et al., 1992) indicate that receptor-antibody complexes are stable at pH >3.5, and are therefore intact even at the lowest lysosomal pH (pH ~4.5). This observation has been confirmed by other investigators (Field et al., 1988, vonZastrow and Kobilka, 1994). Thus visualizing anti-receptor antibody

should be useful technique to follow receptor throughout intracellular trafficking.

Our data indicate that receptor internalization is prominent part of the response of the Hm1 receptor to agonist, and that this process is rapid, occurring within minutes of agonist exposure. A mutation in the third cytoplasmic loop of Hm1 which is intact in coupling but results in internalization deficiency by ligand binding, actually only delays internalization. Mutations which result in a complete defect in both coupling and internalization however, block receptor redistribution and internalization both at rest and in response to agonist. The possibility that the latter mutation results in a profound delay in internalization, rather than a total block, has not been excluded. We present data to suggest that Hm1 may be a recycling receptor, similar to the model of the $\beta_2$AR (vonZastrow and Kobilka, 1994), implying that neurotransmitter receptors of the 7 TMD superfamily may be in a dynamic state, rather than in quiescent, membrane-bound state, in the absence of transmitter or drug. Regulation of these receptors may therefore involve control of recycling kinetics, as well as *in situ* control at the plasma membrane. The mutational analysis we have presented, wherein internalization delay is basis for internalization deficiency, would be consistent with such a kinetic control. Regulation of receptor trafficking which involves a series of stepwise controls has been proposed for other systems (Roach, 1991) and might offer the necessary tight control to implement kinetic control of trafficking.

TABLE I. Binding and functional properties of Hm1, and epitope-tagged Hm1 in HEK 293 cells. A significance value of $p < 0.05$ is indicated by an asterisk (*).

| | **EE-Hm1** | **Hm1** |
|---|---|---|
| Sites/cell | $4.8 \times 10^5$ | $3.9 \times 10^5$ |
| [$^3$H]-NMS Binding | | |
| $B_{max}$ (pmoles/mg) | 3.9 | 3.2 |
| Displacement of [$^3$H]-NMS | | |
| IC50 (mM carbachol) | 3.3 ± 0.7* | 1.6 ± 0.4* |
| Phosphoinositide Stimulation | | |
| $E_{max}$ (fold control) (10 μM carbachol) | 15.5 ± 1 | 13 ± 4 |
| EC50 (μM carbachol) | NA | 8.2 ± 4 |

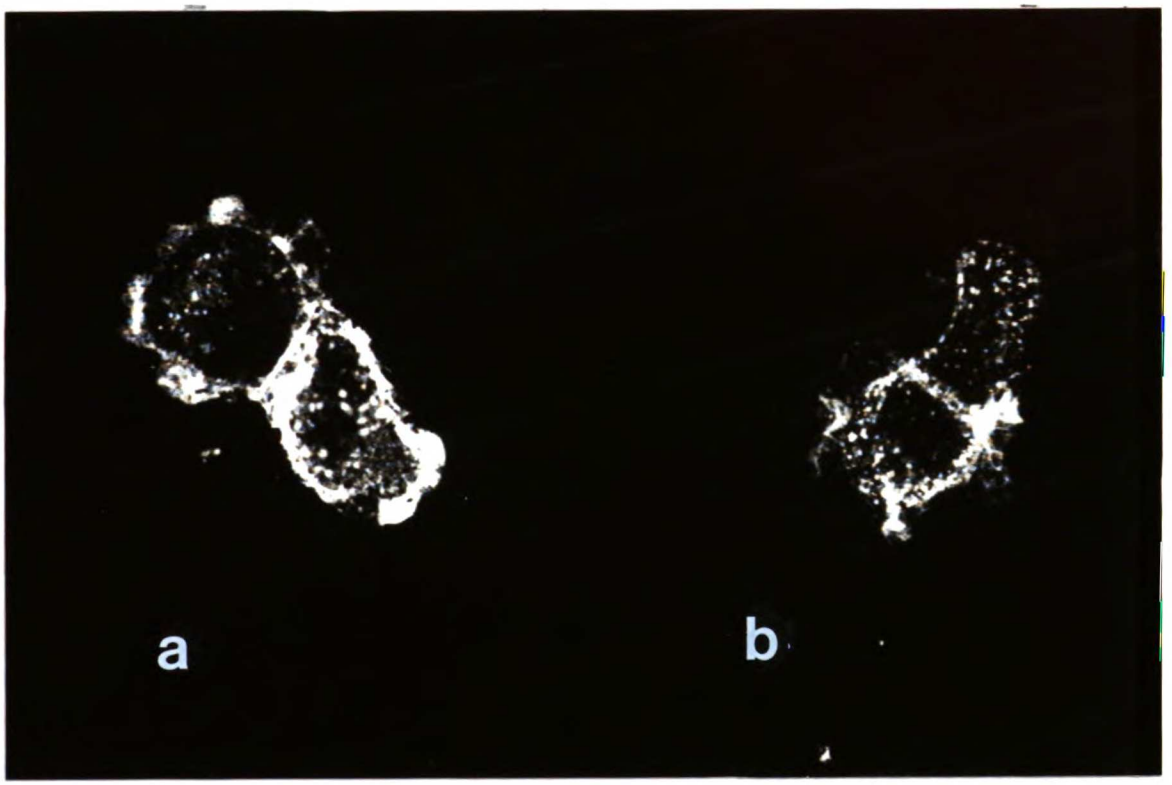


Figure 3.1. Agonist-induced internalization of EE-Hm1. Stably transfected HEK 293 cells were grown on chamber slides as described in "Experimental Procedures" and incubated with buffer or agonist at 37°C for the indicated times prior to fixing and permeabilization. a) no treatment; treated with 1 mM carbachol for b) 5 minutes, c) 10 minutes, d) 15 minutes e) 30 minutes, f) 40 minutes

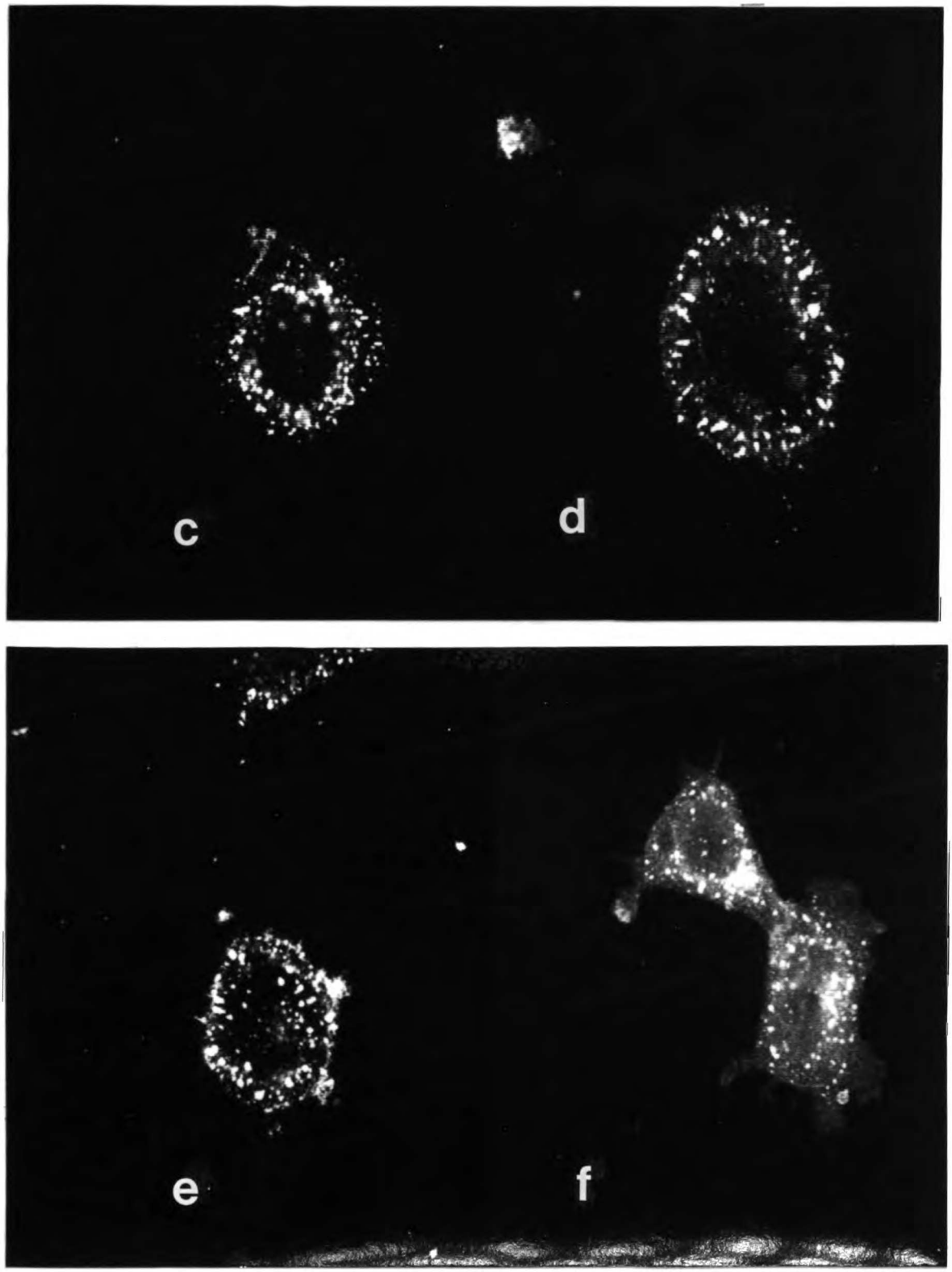


Figure 3.1 (continued)

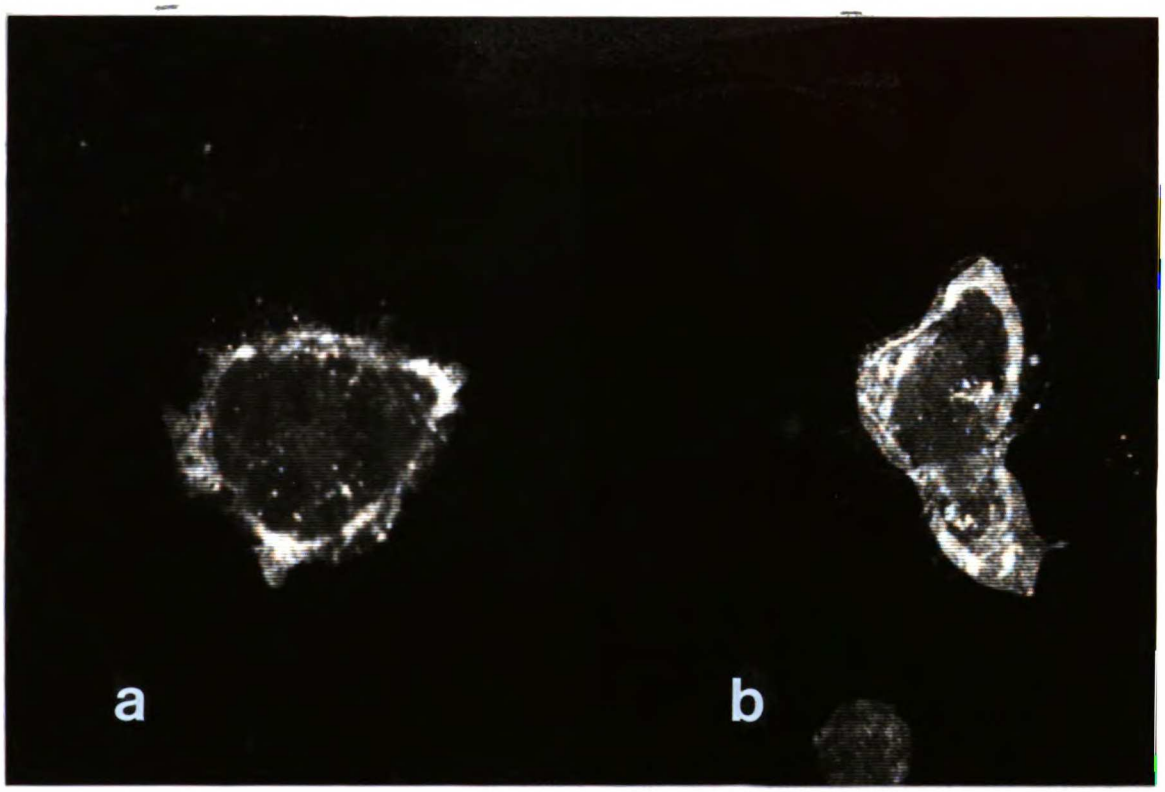


Figure 3.2. Agonist-induced internalization of EE-(d232-358). Cells stably expressing the i3-loop deletion mutant (d232-358) were treated as in Figure 1. a) no treatment; treated with 1 mM carbachol for b) 5 minutes, c) 10 minutes, d) 15 minutes, e) 30 minutes, f) 40 minutes.

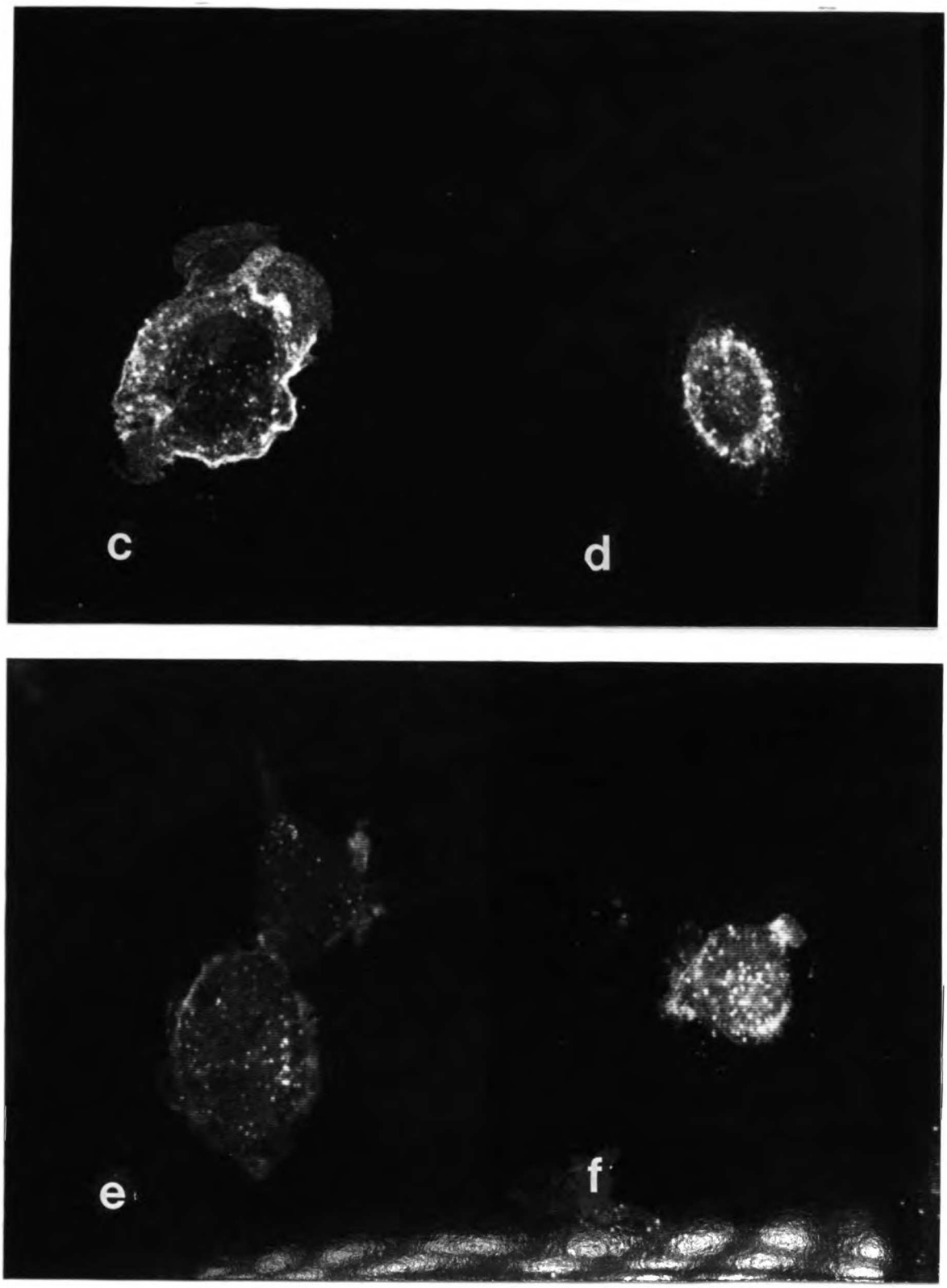


Figure 3.2 (continued)

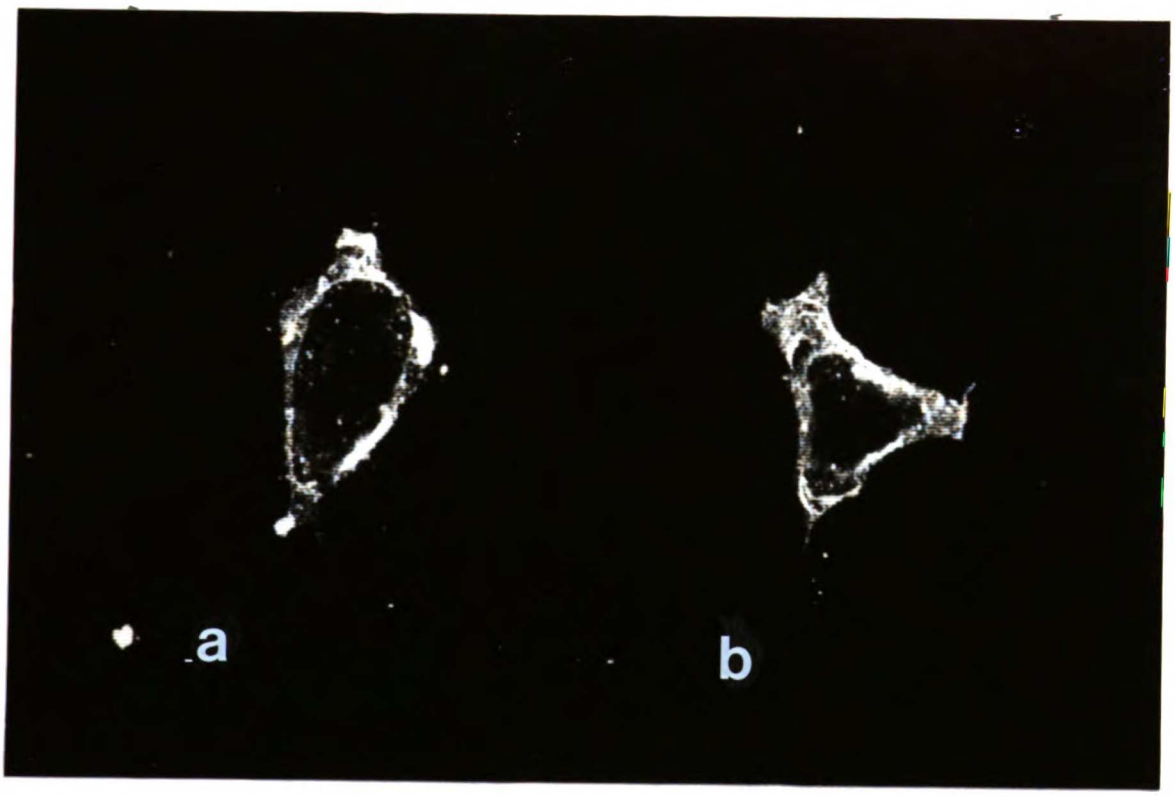


Figure 3.3. Deficient internalization of EE-(V127A/L131A). Cells were treated as in Figures 1-2. a) no treatment, b) 1 mM carbachol for 30 minutes.

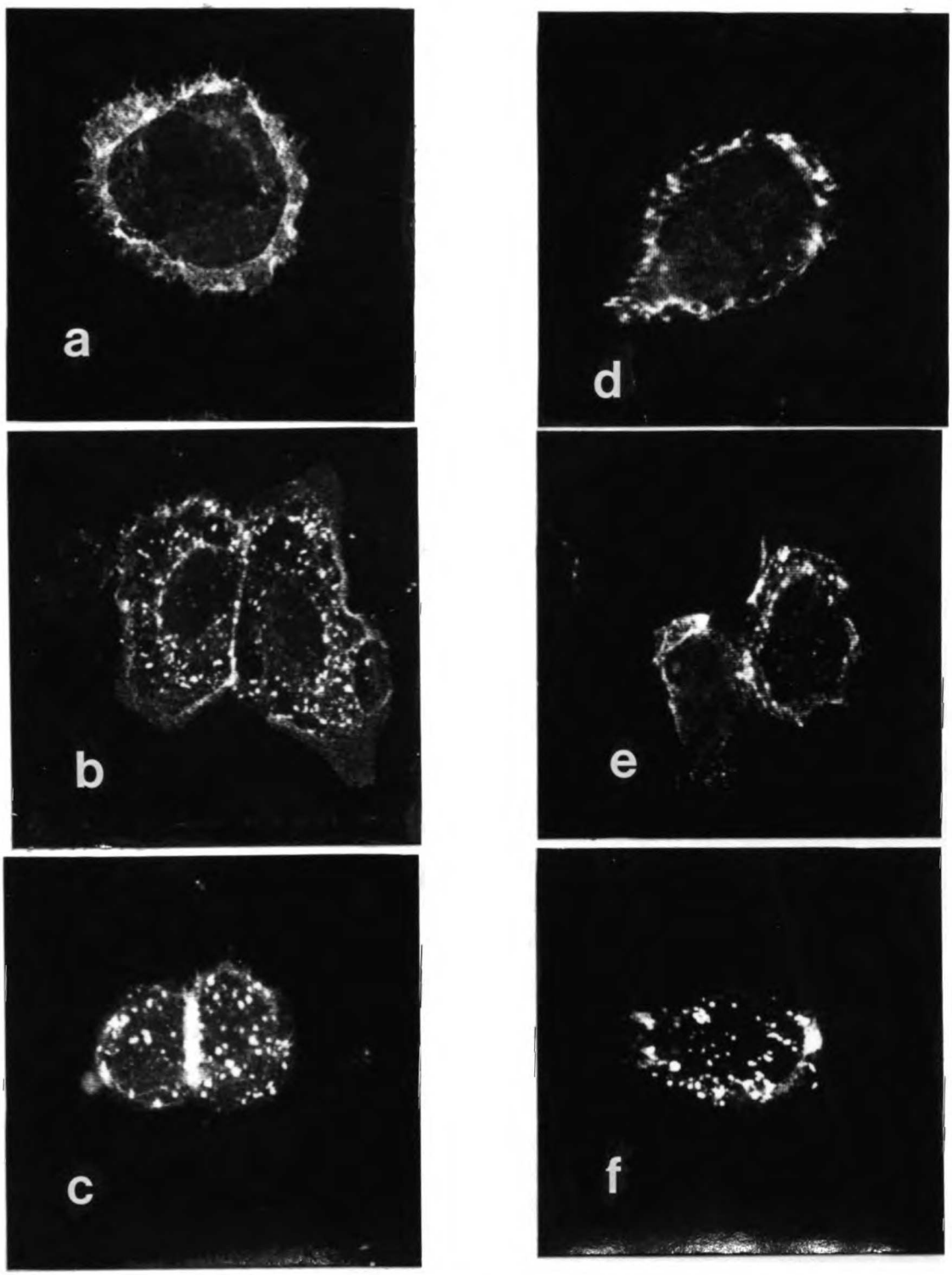


Figure 3.4. Synchronized internalization of EE-Hm1 by temperature shift. EE-Hm1 cells warmed for a) 0 minutes, b) 4 minutes, c) 20 minutes. EE-(d232-358) cells warmed for d) 0 minutes, e) 4 minutes, f) 20 minutes.

# CHAPTER 4

# MUTATIONAL ANALYSIS OF THIRD CYTOPLASMIC LOOP DOMAINS IN G-PROTEIN COUPLING OF THE HM1 MUSCARINIC RECEPTOR


## SUMMARY

We measured dose-response curves for carbachol stimulation of phosphatidyl inositol (PI) turnover with mutants of the Hm1 muscarinic cholinergic receptor having various deletions from amino acids 219 to 358 of the large third intracellular (i3) loop (208 to 366). These deletions had only small or no effects on the ability of Hm1 transfected into 293 HEK cells to stimulate PI turnover. This result indicates that only small regions of 9 to 11 amino acids adjacent to transmembrane domains (TMDs) 5 and 6 can be directly involved in G protein coupling. Point mutations were constructed to test the role of charged amino acids in these junctions. A triple point mutation of Hm1 (E214A/ E216K/ E221K), which mimics the charge distribution in Hm2 (negatively coupled to cAMP) over the first 14 amino acids of i3, and a double point mutation in the N-terminal junction, K359A/K361A, both failed to affect carbachol stimulated PI turnover. Therefore, charge distribution in the loop junctions appears to play a minor role in G protein coupling of Hm1 in HEK 293 cells.

## INTRODUCTION

Studies involving mutations of the $\alpha_1$, $\alpha_2$, and $\beta_2$ adrenergic receptors (Cheung et al., 1989, Cotecchia et al., 1990, Kobilka et al., 1988, O'Dowd et al., 1988, Strader et al., 1987), and the m1-3 muscarinic cholinergic receptors (Kubo et al., 1988, Lechleiter et al., 1990, Wess et al., 1990, Wess et al., 1990, Wess et al., 1989) have led to the conclusion that cytoplasmic domains i2, i3, and the carboxy terminal tail are involved in G protein coupling. However, the role of i3 in G protein activation and selectivity appears to be complex. Exchanging i3 loops or selected portions among $\alpha_1$- and $\beta_2$-adrenergic receptors (Cotecchia et al., 1990), m1 muscarinic and $\beta_2$-adrenergic receptors (Wong et al., 1990), m1 and m2 muscarinic receptors (Kubo et al., 1988), and m2 and m3 muscarinic receptors (Lechleiter et al., 1990, Wess et al., 1990, Wess et al., 1990, Wess et al., 1989) all altered the preferred second messenger pathways between the phospholipase C-phosphatidyl inositol pathway (PLC-PI) and the adenylyl cyclase pathway (AC). Experiments with the m1-3 muscarinic receptors have suggested a role for the N-terminal 17 to 21 amino acids of the i3-loop as coupling determinants. A characteristic charge distribution in this region of the i3 loop has been proposed as one determinant which specifies coupling of a subtype to either PLC-PI or AC (Lechleiter et al., 1990, Wess et al., 1990, Wess et al., 1990, Wess et al., 1989). Lechleiter et al. (Wess et al., 1990) have shown that transfer of nine amino acids of m3, located 12 amino acids distal to the N-terminal of i3, confers the ability of m3 to stimulate PLC-PI to the AC-coupled m2 receptor. While these results support the hy-

pothesis that the N-terminal portion of i3 is important to G protein specificity, not all chimeric receptors gave the expected switch of second messenger pathways (Kubo et al., 1988, Lechleiter et al., 1990, Wess et al., 1990, Wess et al., 1990, Wess et al., 1989), and studies of the $\alpha_1$-adrenergic receptor suggest that the N-terminal portion of i3 is not critical to G protein specificity (Cotecchia et al., 1990). These results suggest that other or additional mechanisms play a role. For example, studies with peptides derived from intracellular receptor domains have implicated domains analogous to the C-terminal of the i3 loop in mediating G protein coupling (Okamoto et al., 1990, Okamoto et al., 1991). In the case of the $\beta_2$-adrenergic receptor ($\beta_2$AR), the amino acid motif BBXXB (B: basic amino acid) was proposed to be critical in G protein coupling (Okamoto et al., 1991). A similar domain (KKAAR) is located at amino acids 361-365 near the C-terminal of the i3 loop of Hm1.

We have previously deleted large portions of the i3 loop of Hm1 (Figure 1), between amino acids 219-358, without observing a significant change in the ability of Hm1 to stimulate PI turnover upon carbachol exposure. With dose response curves using small deletion mutants at the i3 loop junctions, we show here that none of these deletions adjacent to the i3 loop junctions significantly affects the ability to stimulate PI turnover. Further, point mutations designed to affect the charge distribution in the N and C terminal i3 junctions of Hm1 also failed to affect PI turnover.

## EXPERIMENTAL PROCEDURE

### Materials

[$^3$H]-N-Methylscopolamine ([$^3$H]-NMS, specific activity, 80 Ci/mmole) and [$^3$H]-inositol phosphate were obtained from Amersham, Arlington, Illinois). Anion exchange resin AG 1-X8, formate form was from BioRad (Hercules, BA). All other reagents were of analytical grade quality.

### Construction and Expression of Hm1 and Mutants

The gene encoding Hm1 was obtained from a human placental genomic library in vector EMBL3 was used to construct the deletion mutants as described previously (Lameh et al., 1992, Maeda et al., 1990). For the construction of point mutations with the use of oligonucleotides (20 mers), Hm1 was transferred to pBluescript SK(+) (Stratagene, La Jolla, California) using *Bam* H1/*Eco* R1, followed by single strand DNA rescue, using the f1 origin and helper phage infection in the presence of dUTP (Kunkel method). Each mutant Hm1 gene was sequenced before transfer to pSG5. HEK 293 cells were transfected by the calcium phosphate precipitation method as described (Lameh et al., 1992).

### Receptor Binding Assay and Data Analysis.

Transfected HEK 293 cells were incubated for 90 min at room temperature with 0.3 nM [$^3$H]-NMS, in the absence or presence of varying concentrations of carbachol as described previously (Lameh et al., 1992, Maeda et al., 1990). The resultant carbachol displace-

ment curves were analyzed by logistic regression to fit the function, $B = B_{max} - [B_{min} * L]/ [IC_{50} + L] + NSB$, when B = tracer bound (in dpm), L = carbachol concentration, NSB-nonspecific binding. [$^3$H]-NMS binding curves were transformed into saturation curves and fitted to the equation, $B = [B_{max} * L]/[L + K_d]$ after subtraction of non-specific binding (measured in the presence of 10 mM atropine). The curves were fitted using non-linear regression analysis of the unweighted data, with the curve fitting program KaleidaGraph.

**Phosphatidyl Inositol (PI) Turnover**

PI turnover was measured by the method of Berridge et al. (Berridge et al., 1982) as described in (Lameh et al., 1992). For the assay of IP, which accounts for most of the released [$^3$H]-inositol phosphate activity, 6-well cell culture dishes (well diameter 3.5 cm) were used. Results were expressed as percent of total $^3$H activity in the inositol phosphates, and the percent values were compared to baseline between carbachol treated and untreated cells to determine fractional stimulation by carbachol. PI stimulation data were analyzed by non-linear regression using the equation $E = [E_{max} * L^n]/(L^n + EC_{50}{}^n)$. Estimates of n were close to one, and therefore, n was fixed to 1 for the values reported in Table I.

## RESULTS

We have previously demonstrated that very large deletions of i3 from residues 219 to 358 had little or no effect on G protein coupling (Lameh et al., 1992, Maeda et al., 1990). We therefore tested additional smaller deletion mutations to assure that the deleted sequences were not functionally replaced by flanking sequences (Figure 1).

At the C terminal end of i3, the small deletion mutant, d344-358, was also capable of maximally stimulating PI turnover following 1 mM carbachol with a small increase in sensitivity to carbachol relative to wild-type (Table I; Figure 4.2). Part of the alteration in carbachol sensitivity of d344-358 may be attributed to its increased affinity for that ligand, as illustrated by the 1.8-fold lower carbachol $IC_{50}$ relative to wild-type receptor (Table I).

At the N-terminal junction of i3, between 17 to 21 amino acids are thought to play a crucial role in determining the second messenger pathway for m1 and m3 (Lechleiter et al., 1990, Wess et al., 1990, Wess et al., 1989). To address this question further, we tested two smaller deletion mutants, d220-314 and d219-231 (Fig. 1) (Lameh et al., 1992), the latter removing only that domain of Hm1 analogous to the domain proposed to direct coupling specificity in Hm3 (Lechleiter et al., 1990). The carbachol dose-response curves are shown in Figure 2. Both of these deletion mutants showed only small (approximately two-fold) changes of the $EC_{50}$ and $E_{max}$ values (Table I). The larger deletion (d220-314) did not appreciably affect receptor affinity for carbachol and NMS. The 12 residue deletion

(d219-231) caused a slightly increased affinity for carbachol (Table I).

Because of the lack of a consensus sequence for G-protein coupling at the N-terminal junction of i3, it has been suggested that the secondary structure ($\alpha$-helix) with a characteristic charge distribution in this region (Cheung et al., 1989) is the crucial feature determining G protein coupling. To examine the influence of grouped negative charges, we constructed the triple point mutation (E214A/E216K/E 221K, Fig. 1). However, it did not differ from wild type in the ability of carbachol to stimulate PI turnover (Table I). We also introduced a double point mutation into the C terminal junction of the i3 loop (K359A/K361A) which eliminated two positive charges and disturbed the motif BBXXB which was previously shown to be required for G protein activation by peptides derived from the equivalent receptor domain of the $\beta_2$AR (Okamoto et al., 1991). However, these drastic charge changes again failed to cause significant changes in the ability of Hm1 to stimulated PI turnover (Table I).

## DISCUSSION

The i3 loop of Hm1 (156 residues from 210-366) is large in comparison to the i3 loop of the $\beta_2$AR (54 residues) and its function has not been well characterized. The i3 loop of Hm1 and shows little sequence identity to analogous domains of other receptors, including receptors of the same subfamily, except at the N- and C-terminal

junctions of the loop (Bonner et al., 1987, Bonner et al., 1988, Peralta et al., 1987). We have shown previously that large deletions of i3 in Hm1 (d219-333, d232-358) do not affect G protein coupling, suggesting that the sequences that interact with G proteins are limited to the smaller regions adjacent to TMD 5 and 6. Alternatively, these large deletions in i3 may have resulted in hybrid sequences which functionally substitute for the deleted sequences. The minimal effect on PI hydrolysis of a smaller deletion near the C-terminal of i3 (d344-358) confirms that residues immediately preceding position 358 are not required for receptor coupling. This suggest in turn that any direct function in G protein coupling at the C terminal junction of i3 is restricted to the 8 amino acids adjacent to TMD 6. This line of reasoning has been born out in mutational analyses of the small TMD-adjoining domains of the β2-adrenergic receptor and the IGF II/Mannose-6-Phosphate receptor, where the BBXXB motif adjacent to the TMD appears to be critical to G-protein coupling (Okamoto et al., 1990, Okamoto et al., 1991).

Our observation of intact coupling following deletion near the N-terminal of i3 (d219-231) supports the conclusion that residues of i3 more than 9 amino acids from TMD 5 are neither required for G protein coupling, nor essential to specifying coupling to PI turnover in Hm1. These findings conflict with the proposals by Wess *et al.* (Wess et al., 1990, Wess et al., 1989) and Lechleiter *et al.* (Lechleiter et al., 1990) who both concluded that the N-terminal domain of i3 carries the coupling specificity for PI turnover, since pathway specificity (PLC-PI or AC) appears to be transferred in parallel with the exchange of this domain between the m2 and m3 receptors. The m3

receptor has similar coupling specificity (PLC-PI) to Hm1. Hm2 can coupled to both AC and PLC-PI with AC the dominant pathway (Lechleiter et al., 1990). It is possible that the Hm2 sequence DKKEPVANQ (220-228), which was exchanged, is required, but not sufficient, for Hm2 to couple to AC, and that an unknown sequence is required for m2 coupling to PLC-PI. If, however, the Hm3 sequence LAGLQASGT (265-273) is not involved in coupling of Hm3 to the PLC-PI pathway, as our results would predict, then when these domains are exchanged between m2 and m3, m2 coupling to AC is disabled and m2 couples only to PLC-PI, while the effect on m3 is negligible and m3 coupling to PLC-PI remains intact.

The small (approximately two-fold) changes of the $EC_{50}$ for mutants d220-314 and d219-231, and the small decrease in $E_{max}$ for d219-231 (Table I), may suggest a slightly reduced potency and efficacy by the smaller deletion. Alternatively, these effects may be attributed to variability among transiently transfected cell preparations. Stable expression of mutant receptors would minimize this variability and permit differentiation of more subtle effects of mutations on coupling.

This triple mutant (E214A/E216K/E 221K) Hm1 receptor displays a net change of five charges by eliminating three glutamates (E) and introducing two lysines (K), thereby mimicking exactly the charge distribution of Hm2, which is coupled to adenylyl cyclase. The lack of effect of this drastic charge restructuring on G-protein coupling suggests that the secondary structure in this region has no effect on coupling.

The experiments described were performed in transiently transfected cells. Variability in values of maximal PI stimulation which we observed in this study can be related to several factors including differences in cell viability, differences in transfection efficiency, differences in the level of expression resulting from the mutation, as well as other factors unrelated to the mutations. Basal activity is enhanced in transfected cells, which may also result in fluctuations of the ratio values expressing $E_{max}$. Detection of relatively small differences in overall efficacy in any of the mutants would require multiple determinations or selection of stably transfected clones with a constant, defined number of expressed receptors.

In summary, deletions of most of the i3-loop and drastic charge redistribution at its N- and C-terminal junctions failed to affect PI release by Hm1 in HEK 293 cells. These results argue against the hypothesis that the i3 loop of Hm1 is a unique mediator of G protein coupling in HEK 293 cells. Several recent findings are compatable with the data presented here. Data from chimeric muscarinic and β-adrenergic receptors strongly suggest that G protein specificity is dependent on multiple regions of the i2 and i3 loops of these receptors, rather than on the i3 loop alone (Wong and Ross, 1994). The complexity of the coupling domain is also implied by the finding that a point mutation of the $\alpha_2$-AR selectively uncoupled only one of two recognized signaling pathways (Surprenant et al., 1992). Finally, Cheung et al. (Cheung et al., 1989) has demonstrated that hydrophobic, but not hydrophilic, amino acids of the N-terminal i3 junction of the $\beta_2$AR play a significant role in G protein activation. Taken together, these results suggest that the coupling site for G proteins in

the 7 TMD receptors will be composed of a combination of multiple smaller domains in the cytoplasmic loops of these receptors. Moreover, the determinants of G protein subtype specificity within these domains are likely to be subtle, so that small modifications of receptor sequence will direct different G protein specificity. Defining a signal which is composed of multiple, discrete units widely separated in a protein sequence is a daunting prospect at the present time, and will be greatly facilitated by defining the higher order structure of the G protein-coupled receptors.

TABLE I. Inositol phosphate stimulation in deletion mutants of Hm1 as expressed in HEK 293 cells. Individual values for each experiment are listed. $E_{max}$ refers to the fractional increase in PI hydrolysis over baseline. The $EC_{50}$ values represent carbachol stimulation of PI hydrolysis. $IC_{50}$ values (± SD) are for carbachol displacement of [$^3$H]-NMS, and $B_{max}$ represents [$^3$H]-NMS binding.

| **Mutation** | **PI Hydrolysis** | | **Ligand Binding** | |
|---|---|---|---|---|
| | **$E_{max}$** | **$EC_{50}$** (mM) | **$IC_{50}$** (mM carbachol) | **$B_{max}$** (fmoles/mg protein) |
| d220-314 | 1 1 | 1 8 | 0.74 ± 0.2 | 873 ± 112 |
| d219-231 | 7.8,6.1 | 25,19 | 0.19 ± 0.08 | 814 ± 56 |
| d344-358 | 8.4,8.1 | 6.6 | 0.29 ± 0.04 | 580 ± 99 |
| E214A/E216K/E221K | 1 3 | 6.0 | ND | 407 ± 22 |
| K359A/K361A | 9.0 | 17.3 | ND | 781 ± 80 |
| Hm1 (Mean ± SD) | 13 ± 4 | 8.2 ± 4 | 0.53 ± 0.14 | 729 ± 347 |

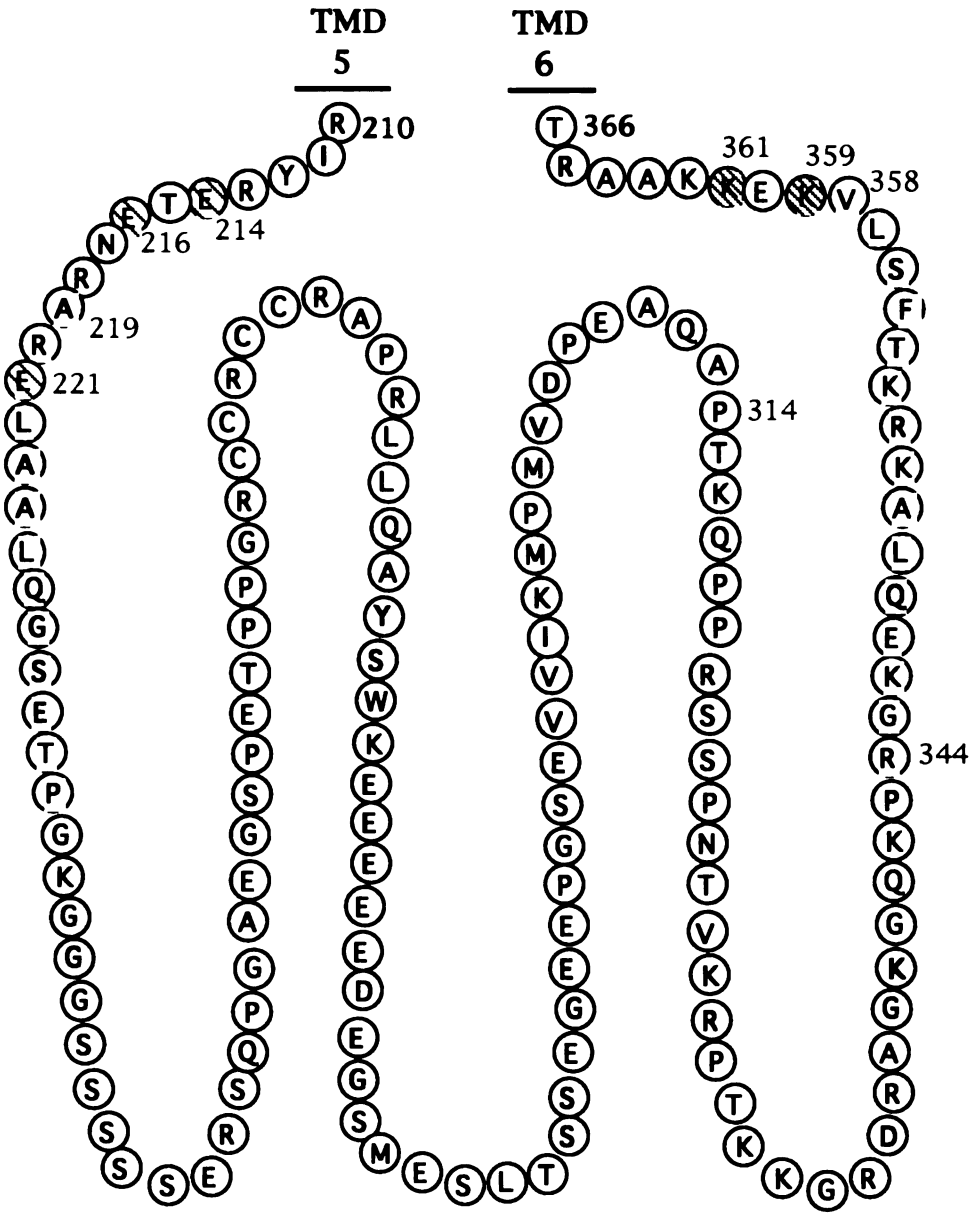


Figure 4.1. Amino acid sequence of the third cytoplasmic loop of Hm1. The deletion and point mutations are as described in the text and in Table I.

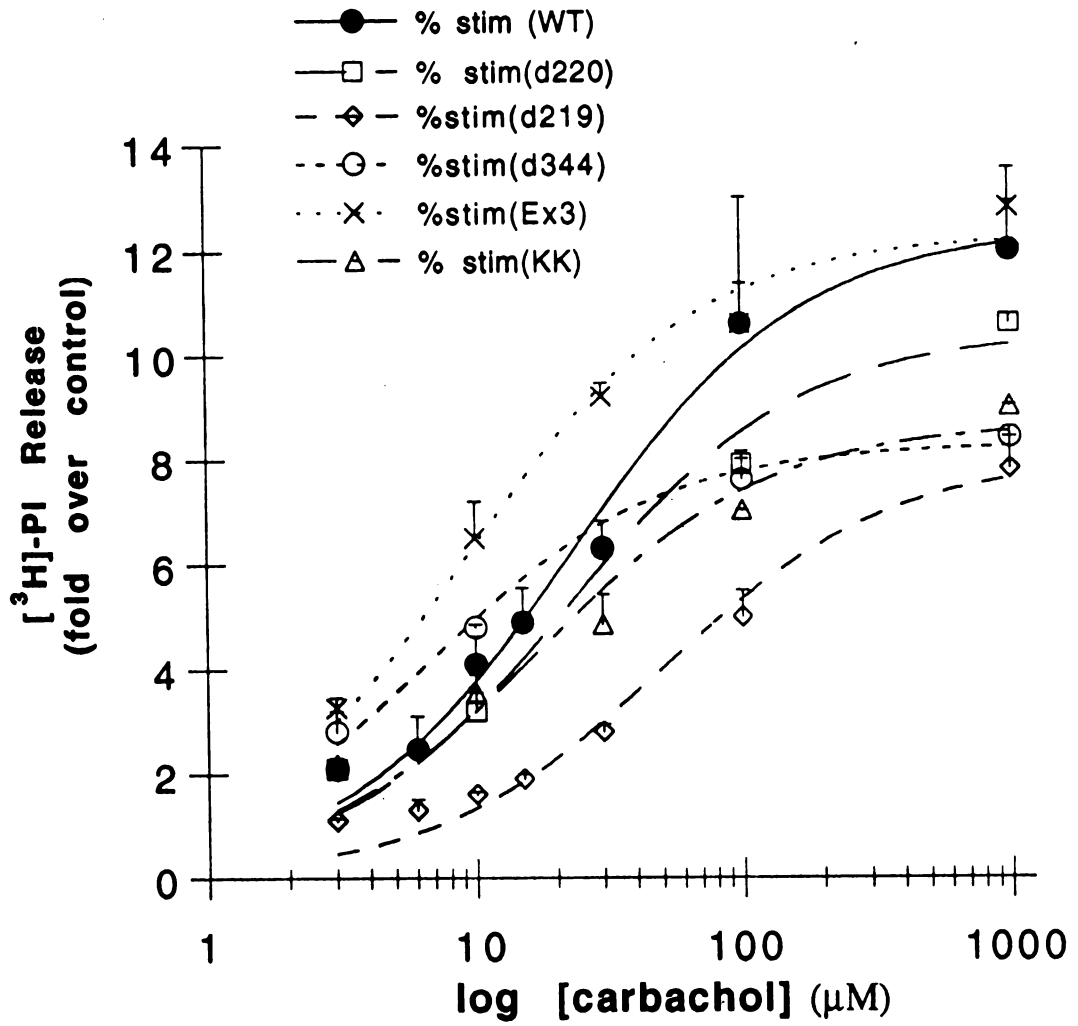


Figure 4.2. Dose-response curve for PI hydrolysis in transfected HEK 293 cells. Cells were labeled with $^{3}$H-*myo* inositol as described in Experimental Procedures and incubated with the concentrations of carbachol indicated. Key to mutants shown in inset.

## REFERENCES


Arden J., Nagata O., Shockley M., Philip M., and Lameh J. (1992) Mutational analysis of the third cytoplasmic loop domains in G-protein coupling of the Hm1 muscarinic receptor. *Biochemical and Biophysical Research Communications* **188,** 1111-1118.

Baumhaker Y., Gafni M., Keren O., and Sarne Y. (1993) Selective and interactive down-regulation of μ- and δ-opioid receptors in human neuroblastoma SK-N-SH cells. *Mol. Pharmacol.* **44,** 461-467.

Berridge M. J., Downes C. P., and Hanley M. R. (1982) Lithium amplifies agonist-dependent phosphoinositol responses in brain and salivary glands. *Bichemical Journal* **206,** 587-595.

Birnbaumer T. L., Abramowitz J., and Brown A. M. (1990) Receptor-effector coupling by G proteins. *Biochem. Biophys. Acta* **1031,** 163-224.

Bonner T. I., Buckley N. J., Young A. C., and Brann M. R. (1987) Identification of a family of muscarinic acetylcholine receptor genes. *Science* **237,** 527-532.

Bonner T. I., Young A. C., Brann M. R., and Buckley N. J. (1988) Cloning and expression of the human and rat m5 muscarinic acetylcholine receptor genes. *Neuron* **1,** 403-410.

Bradford M. M. (1976) A rapid and sensitive method for the quantitation of microgram quantities of protein utilizing the principle of protein-dye binding. *Anal. Biochem.* **72,** 248-254.

Brown A. M., and Birnbaumer L. (1990) Ion channels and their regulation by G protein subunits. *Annual Review of Physiology* **52,** 197-213.

Buckley N. J., Bonner T. I., and Brann M. R. (1988) Localization of a family of muscarinic receptor mRNAs in rat brain. *J. Neurosci.* **8,** 4646-4652.

Carter B. D., and Medzihradsky F. (1993) $G_o$ mediates the coupling of the μ opioid receptor to adenylyl cyclase in cloned neural cells and brain. *Proc. Natl. Acad. Sci. U.S.A.* **90,** 4062-4066.

Chen Y., Mestek A., Liu J., Hurley J. A., and Yu L. (1993) Molecular cloning and functional expression of a μ-opioid receptor from rat brain. *Mol. Pharmacol.* **44,** 8-12.

Cheung A. H., Sigal I. S., Dixon R. A. F., and Strader C. D. (1989) Agonist-promoted sequestration of the $\beta_2$-adrenergic receptor requires regions involved in functional coupling to $G_s$. *Mol. Pharmacol.* **34,** 132-138.

Cone R. I., Lameh J., and Sadee W. (1991) Rapid agonist-induced loss of $^{125}$I-β-endorphin opioid receptor sites in NG108-15, but not SK-N-SH neuroblastoma cells. *Life Sci.* **49,** 147-152.

Cote T., Gosse M. E., and Weems H. B. (1993) Solubilization of high-affinity, guanine nucleotide-selective μ-opioid receptors from 7315c cell membranes. *J. Neurochem.* **61,** 973-978.

Cotecchia S., Exum S., Caron M. G., and Lefkowitz R. J. (1990) Regions of the $\alpha_1$-adrenergic receptor involved in coupling to phosphatidylinositol hydrolysis and enhanced sensitivity of biological function. *Proc. Natl. Acad. Sci. U.S.A.* **87,** 2896-2900.

Curtis C. A. M., Mark Wheatley S. B., Birdsall N. J. M., Eveleigh P., Pedder E. K., Poyner D., and Hulme E. C. (1989) Propylbenzilylcholine mustard labels an acidic residue in transmembrane helix 3 of the muscarinic receptor. *J. Biol. Chem.* **264,** 489-495.

Dixon R. A., Kobilka B. K., Strader D. J., Benovic J. L., Dohlman H. G., Frielle T., Bolanowski M. A., Bennett C. D., Rands E., Diehl R. E., Mumford R. A., Slater E. E., Sigal I. S., Caron M. G., Lefkowitz R. J., and Strader C. D. (1986) Cloning of the gene and cDNA for mammalian beta-adrenergic receptor and homology with rhodopsin. *Nature* **321,** 75-79.

Engelman D. M., Henderson R., McLachlan A. D., and Wallace B. A. (1980) Path of the polypeptide in bacteriorhodopsin. *Proc. Natl. Acad. Sci. U.S.A.* **77,** 2023-2027.

Eppler C. M., Hulmes J. D., Wang J.-B., Johnson B., Corbett M., Luthin D. R., Uhl G. R., and Linden J. (1993) Purification and partial amino acid sequence of a μ opioid receptor from rat brain. *J. Biol. Chem.* **268,** 26447-26451.

Field J., Nikawa J., Broek D., MacDonald B., Rodgers L., Wilson I. A., Lerner R. A., and Wigler M. (1988) Purification of a RAS-responsive adenylyl cyclase complex from Saccharomyces cerevisiae by use of an epitope addition method. *Molecular Cell Biology* **8,** 2159-2165.

Fukuda K., Kato S., Mori K., Nishi M., and Takeshima H. (1993) Primary structure and expression from cDNA of rat opioid receptor delta- and mu-subtypes. *FEBS Lett.* **327,** 311-314.

Fukuda K., Kubo T., Akiba I., Maeda A., Mishina M., and Numa S. (1987) Molecular distinction between muscarinic acetylcholine receptor subtypes. *Nature* **327,**

Ghinea N., Hai M. T. V., Picard M.-T. G., Houllier A., and Schoevaert D. (1992) Pathways of internalization of the hCG/LH receptor: Immunoelectron microscopic studies in Leydig cells and transfected L-cells. *J. Cell Biol.* **118,** 1347-1358.

Glantz S. (1981) *Primer of Biostatistics*, pp 70-71. McGraw-Hill, New York.

Grussenmeyer T., Scheidtmann K. H., Hutchinson M. A., Eckhart W., and Walter G. (1985) Complexes of polyoma medium T antigen and cellular proteins. *Proc. Natl. Acad. Sci. U.S.A.* **82,** 7952-7954.

Haga K., and Haga T. (1985) Purification of the muscarinic acetylcholine receptor from porcine brain. *J. Biol. Chem.* **260,** 7927-7935.

Haga K., and Haga T. (1992) Activation by G protein βγ subunits of agonist- or light-dependent phosphorylation of muscarinic acetylcholine receptors and rhodopsin. *J. Biol. Chem.* **267,** 2222-2227.

Haga K., Haga T., and Ichiyama A. (1990) Phosphorylation by protein kinase C of the muscarinic acetylcholine recepor. *J. Neurochem.* **54,** 1639-1644.

Harada H., Ueda H., Katada T., Ui M., and Satoh M. (1990) Phosphorylated μ opioid receptor purified from rat brain lacks functional coupling with Gi1, a GTP-binding protein in reconstituted lipid vessicles. *Neurosci. Lett.* **113,** 47-49.

Harada H., Ueda H., Wada Y., Katada T., Ui M., and Satoh M. (1989) Phosphorylation of μ-opioid receptors-a putative mechanism of selective uncoupling of receptors-Gi interaction, measured with low $K_m$

GTPase and nucleotide-sensitive agonist binding. *Neurosci. Lett.* **100,** 221-226.

Harden T. K., Petch L. A., Traynelis S. F., and Waldo G. L. (1985) Agonist-induced alteration in the membrane form of muscarinic receptors. *J. Biol. Chem.* **260,** 13060-13066.

Hassan A. H. S., Almeida O. F. X., Gramsch C., and Herz A. (1989) Immunocytochemical demonstration of the opioid receptors in selected rat brain areas and neuroblastoma x glioma hybrid (NG108-15) cells using monoclonal anti-idiotypic antibody. *Neurosci.* **32,** 269-278.

Hasselmo M. E., and Bower J. M. (1993) Acetylcholine and memory. *TINS* **16,** 218-222

Hausdorff W. P., Bouvier M., O'Dowd B. F., Irons G. P., Caron M. G., and Lefkowitz R. J. (1989) Phosphorylation sites on two domains of the β2-adrenergic receptor are involved in distinct pathways of receptor desensitization. *J. Biol. Chem.* **244,** 12657-126665.

Hausdorff W. P., Campbell P. T., Ostrowski J., Yu S. S., Caron M. G., and Lefkowitz R. J. (1991) A Small region of the b-adrenergic receptor is selectively involved in its rapid regulation. *Proc. Natl. Acad. Sci. U.S.A.* **88,** 2979-2983.

Hausdorff W. P., Caron M. G., and Lefowitz R. J. (1990) Turning off the signal: desensitization of β-adrenergic receptor function. *FASEB J.* **4,** 2881-2889.

Hausdorff W. P., Lohse M. J., Bouvier M., Liggett S. B., Caron M. G., and Lefkowitz R. J. (1990) Two kinases mediate agonist-dependent phosphorylation and desensitization of the beta-2 adrenergic receptor. *Symposia of the Society for Experimental Biology* **44,** 225-240.

Hille B. (1992) G Protein-coupled mechanisms and nervous signaling. *Neuron* **9,** 187-195.

Kobilka B. K., Kobilka T. S., Daniel K., Regan J. W., Caron M. G., and Lefkowitz R. J. (1988) Chimeric $\alpha_2$-,$\beta_2$-adrenergic receptors: delineation of domains involved in effector coupling and ligand binding specificity. *Science* **240,** 1310-1316.

Koenig J. A., and Edwardson J. M. (1994) Kinetic analysis of the trafficking of muscarinic acetylcholine receptors between the plasma membrane and intracellular compartments. *J. Biol. Chem.* **269,** 17174-17182.

Kubo T., Bujo H., Akiba I., Nakai J., Mishina M., and Numa S. (1988) Location of a region of the muscarinic acetylcholine receptor involved in selective effector coupling. *FEBS Lett.* **241,** 119-125.

Kubo T., Fukuda K., Mikami A., Maeda A., Takahashi H., Mishima M., Haga T., Haga K., Ichiyama A., Kangawa K., Kojima M., Matsuo H., Hirose T., and Numa S. (1986) Cloning, sequencing and expression of complementary DNA encodong the muscarinic acetylcholine receptor. *Nature* **323,** 411-416.

Kwatra M. M., Benovic J. L., Caron M. G., and Lefkowitz R. J. (1989) Phosphorylation of chick heart muscarinic cholinergic receptors by the β-adrenergic receptor kinase. *Biochemistry* **28,** 4543-45347.

Lameh J., Cone R. I., Maeda S., Philip M., Corbain M., Nadasdi L., Ramachandran J., Smith G. M., and Sadée W. (1990) Structure and function of G-protein coupled receptors. *Pharmaceutical Research* **7,** 1213-1221.

Lameh J., Philip M., Sharma Y. K., Moro O., Ramachandran J., and Sadee W. (1992) Hm1 Muscarinic Cholinergic Receptor Internalization Requires a Domain in the Third Cytoplasmic Loop. *J. Biol. Chem.* **267,** 13406-13412.

Lechleiter J., Hellmiss R., Duerson K., Ennulat D., David N., Clapham D., and Peralta E. (1990) Distinct sequence elements control the specificity of G protein activation by muscarinic acetylcholine receptor subtypes. *EMB O J.* **9,** 4381-4390.

Lefkowitz R. J. (1993) G Protein-Coupled Receptor Kinases. *Cell* **74,** 409-412.

Liles W. C., Hunter D. D., Meier K., and Nathanson N. M. (1985) Activation of protein kinase C induces rapid internalization and subsequent degradation of muscarinic acetylcholine receptors in neuroblastoma cells. *J. Biol. Chem.* **261,** 5307-5313.

Loh H. H., and Smith A. P. (1990) Molecular characterization of the opioid receptor. *Annual Review of Pharmacology and Toxicology* **30,** 123-147.

Lohse M. J., Benovic J. L., Codina J., Caron M. G., and Lefkowitz R. J. (1990) β-Arrestin: A protein that regulates β-adrenergic receptor function. *Science* **248,** 1550-1553.

Maeda S., Lameh J., Mallet W., Philip M., Ramachandran J., and Sadee W. (1990) Internalization of the Hm1 muscarinic cholinergic receptor involves the third cytoplasmic loop. *FEBS Lett.* **269,** 386-388.

Maloteaux J. M., and Hermans E. (1994) Agonist-induced muscarinic receptor internalization, recycling and degradation in cultured neuronal cells. *Biochemical Pharmacology* **45,** 77-88.

Mayanil C. S. K., Richardson R., and Hosey M. M. (1989) Subtype-specific antibodies for muscarinic cholinergic receptors. I. Characterization using transfected cells and avian and mammalian cardiac membranes. *Mol. Pharmacol.* **40,** 900-907.

Moro O., Lameh J., Hogger P., and Sadee W. (1993) Hydophobic amino acid in the i2 loop plays a key role in receptor-G protein coupling. *J. Biol. Chem.* **268,** 22273-22278.

Moro O., Lameh J., and Sadee W. (1994) Serine- and Theonine-rich Domain Regulates Internalization of Muscarinic Cholinergic Receptors. *J. Biol. Chem.* **269,** 6651-6655.

Moro O., Shockley M. S., Lameh J., and Sadée W. (1994) Overlapping multi-site domains of the muscarinic cholinergic Hm1 receptor involved in signal transduction and sequestration. *J. Biol. Chem.* **269,** 6651-6655.

Nathans J., and Hogness D. S. (1984) Isolation and nucleotide sequence of the gene encoding human rhodopsin. *Proc. Natl. Acad. Sci. U.S.A.* **81,** 4851-4855.

Nestler E. (1992) Molecular Mechanism of Drug Addiction. *J. Neurosci.* **12,** 2439-2450.

North R. A., Williams J. T., Surprenant A., and Christie M. J. (1987) Mu and delta receptors belong to a family of receptors that are coupled to potassium channels. *Proc. Natl. Acad. Sci. U.S.A.* **84,** 5487-5491.

O'Dowd B. F., Hnatowich M., Regan J. W., Leader W. M., Caron M. G., and Lefkowitz R. J. (1988) Site-directed mutagenesis of the cytoplasmic domains of the human $\beta_2$-adrenergic receptor: Localization of

regions involved in G protein-receptor coupling. *J. Biol. Chem.* **263,** 15985-15992.

Ofri D., Ritter A. M., Liu Y., Gioannini T. L., Hiller J. M., and Simon E. J. (1992) Characterization of solubilized opioid receptors: reconstitution and uncoupling of guanine nucleotide-sensitive agonist binding. *J. Neurochem.* **58,** 628-635.

Okamoto T., Katada T., Murayama Y., Ui M., Ogata E., and Nishimoto I. (1990) A Simple structure encodes G protein-activating function of the IGF-II/ Mannose 6-phosphate receptor. *Cell* **62,** 709-717.

Okamoto T., Murayama Y., Hayashi Y., Inagaki M., Ogata E., and Nishimoto I. (1991) Identification of a $G_s$ activator region of the $\beta_2$-adrenergic receptor that is autoregulated via protein kinase A-dependent phosphorylation. *Cell* **67,** 723-730.

Ornatowska M., and Glasel J. A. (1992) Two- and three-dimensional distributions of opioid receptors on NG108-15 cells visualized with the aid of fluorescence confocal microscopy and anti-idiotypic antibodies. *J. Chem. Neuroanat.* **5,** 95-106.

Ovchinnikov Y. A., Abdulaeh N. G., Feigina M. Y., Artamonov I. D., Zolotereve A. S., Kostina M. B., Bogachuk A. S., Miroshnikov A. I., Martinov V. I., and Kudelin A. B. (1882) The complete amino acid sequence of visual rhodopsin. *Bioorganic Khim* **8,** 1011-1014.

Peralta E. G., Ashkenazi A., Winslow J. W., Smith D. H., Ramachandran J., and Capon D. J. (1987) Distinct primary structures, ligand binding properties and tissue-specific expression of four human muscarinic acetylcholine receptors. *EMB O J.* **6,** 3923-3929.

Probst W. C., Snyder L. A., Schuster D. I., Brosius J., and Sealfon S. C. (1992) Sequence alignment of the G-protein coupled receptor superfamily. *DNA and Cell Biology* **11,** 1-20.

Raposo G., Dunia I., Delavier-Klutchko C., Kaveri S., and Strosberg A. D. (1989) Internalization of b-adrenergic receptor in A431 cells involves non-coated vesicles. *European Journal of Cell Biology* **50,** 340-352.

Raposo G., Dunia I., Marullo S., Andre C., Guillet J.-G., Strosberg A. D., Benedetti E. L., and Hoebeke J. (1987) Redistriburion of muscarinic acetylcholine receptors on human fibroblasts induced by regulatory ligands. *Biol. Cell* **60,** 117-123.

Raymond J. R. (1991) Protein Kinase C Induces Phosphorylation and Desensitization of the Human 5-$HT_{1A}$ Receptor. *J. Biol. Chem.* **266,** 14747-14753.

Raynor K., Kong H., Chen Y., Yatsuda K., Yu L., Bell G., and Reisine T. (1994) Pharmacological characterization of the cloned κ–, δ–, and μ-Opioid receptors. *Mol. Pharmacol.* **45,** 330-334.

Richardson R., and Hosey M. M. (1992) Agonist-induced phosphorylation and desensitization of human m2 muscarinic cholinergic receptors in Sf9 insect cells. *J. Biol. Chem.* **267,** 22249-22255.

Richardson R., Mayanil C. S. K., and Hosey M. M. (1991) Subtype-specific antibodies for muscarinic cholinergic receptors. II. Studies with reconstituted chick heart receptors and the GTP-binding protein $G_o$. *Mol. Pharmacol.* **40,** 908-914.

Richardson R. M., and Hosey M. M. (1990) Agonist-induced phosphorylation of purified cardiac muscarinic cholinergic receptors by protein kinase C. *Biochemistry* **29,** 8555-8561.

Roach P. J. (1991) Multisite and Hierarchal Protein Phosphorylation. *J. Biol. Chem.* **266,** 14139-14142.

Schroeder J. E., Fischbach P. S., Zheng D., and McCleskey E. W. (1991) Activation of μ opioid Receptors inhibits transient high- and low-threshold $Ca^{2+}$ currents, but spares a sustained current. *Neuron* **6,** 13-20.

Sharma S. K., Nirenberg M., and Klee W. A. (1975) Morphine receptors as regulators of adenylate cyclase. *Proc. Natl. Acad. Sci. U.S.A.* **72,** 590-4.

Slowiejko D. M., Levey A. I., and Fisher S. K. (1994) Sequestration of muscarininc cholinergic receptors in permeabilized neuroblastoma cells. *J. Neurochem.* **62,** 1795-1803.

Strader C. D., Dixon R. A. F., Cheung A. H., Candelore M. r., Blake A. D., and Sigal I. S. (1987) Mutations that uncouple the β-adrenergic receptor from $G_s$ and increase agonist affinity. *J. Biol. Chem.* **262,** 16439-16443.

Surprenant A., Horstman D. A., Akbarali H., and Limbird L. E. (1992) A point mutation in the a2-adrenoceptor that blocks coupling to potassium but not calcium currents. *Science* **257,** 997-980.

Thompson R. C., Mansour A., Akil H., and Watson S. J. (1993) Cloning and pharmacological characterization of a rat μ opioid receptor. *Neuron* **11,** 903-913.

Tobin A. B., and Nahorski S. R. (1993) Rapid agonist-mediated phosphorylation of the m3-muscarinic receptor revealed by immunoprecipitation. *J. Biol. Chem.* **268,** 9817-9823.

Toll L. (1992) Comparison of mu opioid receptor binding on intact neuroblastoma cells with guinea pig brain and neuroblastoma cell membranes. *J. Pharmacol. Exp. Ther.* **260,** 9-15.

Trowbridge I. S. (1991) Endocytosis and signals for internalization. *Current Opinion in Cell Biologynt* **3,** 634-641.

Uchiyama H., Ohara K., Haga K., Haga T., and Ichiyama A. (1990) Location in muscarinic acetylcholine receptor of sites for [$^3$H]-propylbenzilylcholine mustard binding and for phosphorylation with protein kinase C. *J. Neurochem.* **54,** 1870-1881.

Unwin P. N., and Henderson R. (1975) Molecular structure determination by electron microscopy of crystalline specimens. *Journal of Molecular Biology* **94,** 425-440.

vonZastrow M., Duane E. Keith J., and Evans C. J. (1993) Agonist-induced state of the δ-opioid receptor that discriminates between opioid peptides and opiate alkaloids. *Mol. Pharmacol.* **44,** 166-172.

vonZastrow M., and Kobilka B. (1994) Antagonist-dependent- and independent steps in the mechanism of adrenergic receptor internalization. *J. Biol. Chem.* **269,** 18448-18452.

vonZastrow M., and Kobilka B. K. (1992) Ligand-regulated internalzation and recycling of human β2-adrenergic receptors between the plasma membrane and endosomes containing transferrin receptor. *J. Biol. Chem.* **267,** 3530-3538.

vonZastrow M., Link R., Daunt D., Barsh G., and Kobilka B. (1993) Subtype-specific differenced in the intracellular sorting of G protein-coupled receptors. *J. Biol. Chem.* **268,** 763-66.

Wall S. J., Yasuda R. P., Hory F., Flagg S., Martin B., Ginns E., and Wolfe B. B. (1991) Production of antisera selective for m1 muscarinic receptors using fusion proteins: distribution of m1 receptors in rat brain. *Mol. Pharmacol.* **39,** 643-649.

Wang J.-B., Imai Y., Eppler C. M., Spivak C. E., and Uhl G. R. (1993) μ opiate receptor: cDNA cloning and expression. *Proc Nat Acad Sci* **90,** 10230-10234.

Wess J., Bonner T. I., and Brann M. R. (1990) Chimeric m2/m3 muscarinic receptors: role of carboxy terminal receptor domains in selectivity of ligand binding and coupling to phosphoinositide hydrolysis. *Mol. Pharmacol.* **38,** 872-877.

Wess J., Bonner T. I., Dorje F., and Bran M. R. (1990) Delineation of muscarinic receptor domains conferring selectivity of coupling to guanine nucleotide-binding proteins and second messengers. *Mol. Pharmacol.* **38,** 517-523.

Wess J., Brann M. R., and Bonner T. I. (1989) Identification of a small intracellular region of the muscarinic m3 receptor as a determinant of selective coupling to PI turnover. *FEBS Lett.* **258,** 133-136.

Wimpey T. L., and Chavkin C. (1991) Opioids activate both an inward rectifier and a novel voltage-gated potasium conductance in the hippocampal formation. *Neuron* **6,** 281-9.

Wong D., and Brodsky F. M. (1992) 100-kD Proteins of Golgi- and Trans-Golgi Network-Associated Coated Vesicles Have Related But Distinct Membrane Binding Properties. *J. Cell Biol.* **117,** 1171-1179.

Wong S. K.-F., Parker E. M., and Ross E. M. (1990) Chimeric muscarinic cholinergic:b-adrenergic receptors that activate Gs in response to muscarinic agonists. *J. Biol. Chem.* **265,** 6219-6224.

Wong S. K.-F., and Ross E. M. (1994) Chimeric muscarinic cholinergic:β-adrenergic receptors that are functionally promiscuous among G proteins. *J. Biol. Chem.* **269,** 18968-18976.

Yu S. S., Lefkowitz R. J., and Hausdorff W. P. (1993) β-Adrenergic receptor sequestration: a potential mechanism of receptor resensitization. *J. Biol. Chem.* **268,** 337-341.

Yu V., Eiger S., Duan D. S., Lameh J., and Sadee W. (1990) Regulation of cyclic AMP by the mu-opioid receptor in human neuroblastoma SH-SY5Y cells. *J. Neurochem.* **55,** 1390-1396.

Yu V., Richards M., and Sadee W. (1986) A Human neuroblastoma cells line expresses μ and δ Opioid receptor sites. *J. Biol. Chem.* **261,** 1065-1070.

Yu V., and Sadee W. (1988) Efficacy and tolerance of narcotic analgesics at the mu opioid receptor in diferentiated human neuroblastoma cells. *J. Pharmacol. Exp. Ther.* **245,** 350-355.

Zar J. (1974) *Biostatistical Analysis*. pp. 121-124 and p. 413. Prentice-Hall, Englewood Cliffs.

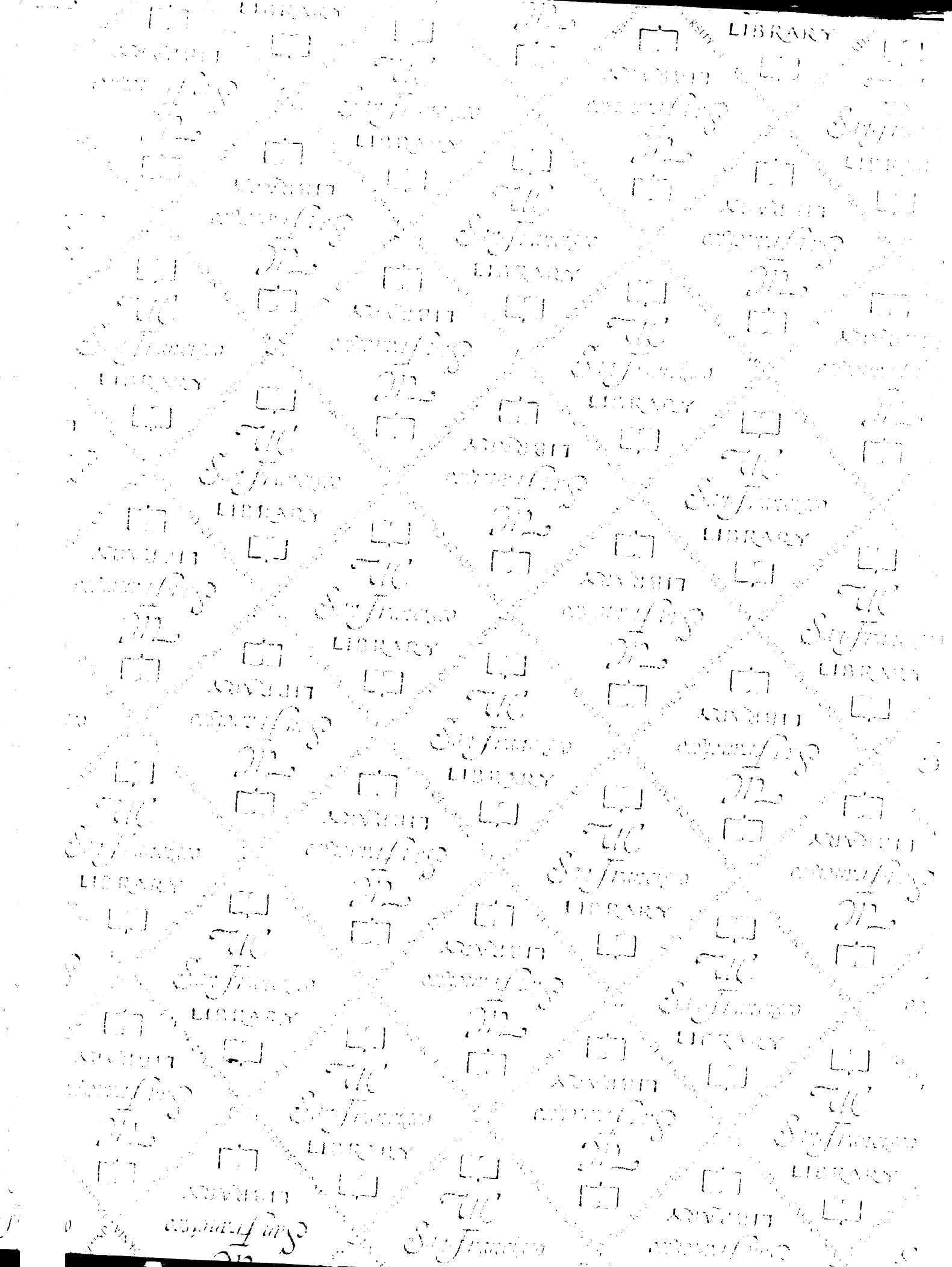
LIBRARY